Phil. Trans. R. Soc. Lond. A. **286**, 527–548 (1977) [527]
Printed in Great Britain

Uranium mineralization of the Witwatersrand and Dominion Reef systems

By P. R. Simpson and J. F. W. Bowles
Institute of Geological Sciences, Geochemical Division, 64–78 Gray's Inn Road, London WC1X 8NG

[Plates 1–10]

Preface

The problem of the origin of the mineralization of the Witwatersrand and Dominion Reef has been one of the great controversies of the past 50 years. Any new attempt to solve it requires the application of the most up-to-date mineralogical techniques including the combined use of ore microscopy with electron microprobe analysis, radioisotope and stable isotope determinations, fission-track studies of uranium distribution, and detailed analysis of fluid inclusions. All these skills have been brought to bear in the work described in this and the two papers following, and although unequivocable results have not yet been obtained, important new information on the bimodal nature of the uranium mineralization has been established.

The significance of this study, which illustrates the application of techniques that will become more commonplace as the 21st century approaches, lies in providing essential information on the origin of uranium in quartz pebble conglomerates. More than 35 % of known uranium reserves occur in such rocks, particularly in Canada and South Africa but also, as recently reported, in Algeria. Previously many geologists have held that uranium can only be enriched to economic grades in Precambrian rocks if anoxygenic atmospheric conditions prevailed at the time of sedimentation. However, the remarkable similarity between the sub-economic concentrations of thorian uraninite in the present-day Indus Valley and that of the Dominion Reef and Witwatersrand System as well as other evidence invalidates any such concept.

Further work is required to complete the story of the Witwatersrand mineralization and it is hoped that multidisciplinary investigations will continue. The full resolution of the genesis of the mineralization could result in new discoveries that are essential to the availability of uranium for future energy needs.

S. H. U. Bowie, F.R.S.

Uranium-bearing minerals in the Witwatersrand and Dominion Reef sediments have been studied by ore microscopic, electron microprobe, fission track and neutron activation analytical methods to determine the controls of uranium mineralization. In the Dominion Reef, which represents a high-energy banket type of depositional environment, allogenic thorian uraninite occurs in hydraulic equivalence with allogenic pyrite, quartz and possibly also gold in the sediments which have uranium–thorium ratios between 3.1 and 5.6 indicating substantial amounts of thorium-rich resistate minerals.

The Witwatersrand sediments have uranium–thorium ratios ranging between 7.1 and 19.6 indicating lesser amounts of resistates which is consistent with the lower-energy depositional environment. The proximal or nearshore deposits are of banket type but are distinguished from the Dominion Reef by the abundance of concretionary pyrite formed within the Basin and the presence of carbonaceous matter. The distal

deposits formed at greater distance from the shoreline contain decaying organic material which has precipitated both uranium and gold from solution. Subsequent metamorphism has resulted in the formation of carbonaceous material bearing finely disseminated low-thorium pitchblende and a fine dissemination of gold associated with sulphides and arsenides.

Further evidence of the existence of uranium in solution is to be found in the banket deposits. In this case fine disseminations of uranium (> 500 parts/10^6) occur in clay minerals within concretionary pyrite nodules and in lenticles formed of clay minerals in Witwatersrand banket deposits. They represent reduction-deposition of the soluble uranyl ion below the sediment–water interface where conditions are reducing.

Allogenic thorian uraninite from the present-day Indus river has a texture, composition and association with gold and pyrite similar to allogenic uraninite in the Witwatersrand and Dominion Reef System. Thorian uraninite is a stable phase over large distances in this river. Hence it would appear quite unnecessary to postulate a reducing atmosphere for the transportation of detrital uraninite. Moreover the retention of sulphate and uranyl ions in solution in the model proposed here suggests that the atmosphere was oxidizing at the time of deposition. This conclusion indicates the likely occurrence in younger sediments of mineralization of this type provided the necessary geological criteria are met.

Introduction

Uranium mineralization in the Witwatersrand and Dominion Reef sediments is presently and has been, since its discovery by Cooper in 1923, the subject of debate and speculation as to its origin.

Mineralization has been described variously as the product of hydrothermal processes by Graton (1930) and sedimentary processes by Ramdohr (1958) and others. The detrital hypothesis for the origin of uraninite has been taken to account for all primary mineralization in the Basin by some workers. This idea has been further developed to the point where a reducing atmosphere was invoked as an essential prerequisite to the transportation of detrital uraninite grains (Liebenberg 1955; Grandstaff 1975). This has led to the notion that uraniferous conglomerates are thereby restricted by these atmospheric conditions to the Archaean or early Proterozoic (Robertson 1974).

The purpose of this study is to re-evaluate the uranium mineralization using mineralogical methods since the implications of the earlier work for the further discovery of uraniferous conglomerates would appear to be unduly restrictive.

All specimens available to the authors were sectioned for study to obtain as broad a view of the principal types of mineralization as possible, though it is appreciated that the coverage of this Basin is by no means as complete as could be wished. The outline geology, principal mining areas, and section numbers of specimens studied, are shown in figures 1 and 2.

In pursuing this investigation, two questions have been uppermost in our minds: firstly, does the formation of these and similar deposits elsewhere require a reducing atmosphere, or merely reducing conditions of deposition beneath the sediment/water interface; and secondly, what are the respective rôles of uranium as detrital grains of uraninite and as uranyl ions in solution. Answers to these two questions will have considerable relevance to the understanding of the mode of formation and estimating the potential for new discoveries of this type of mineralization.

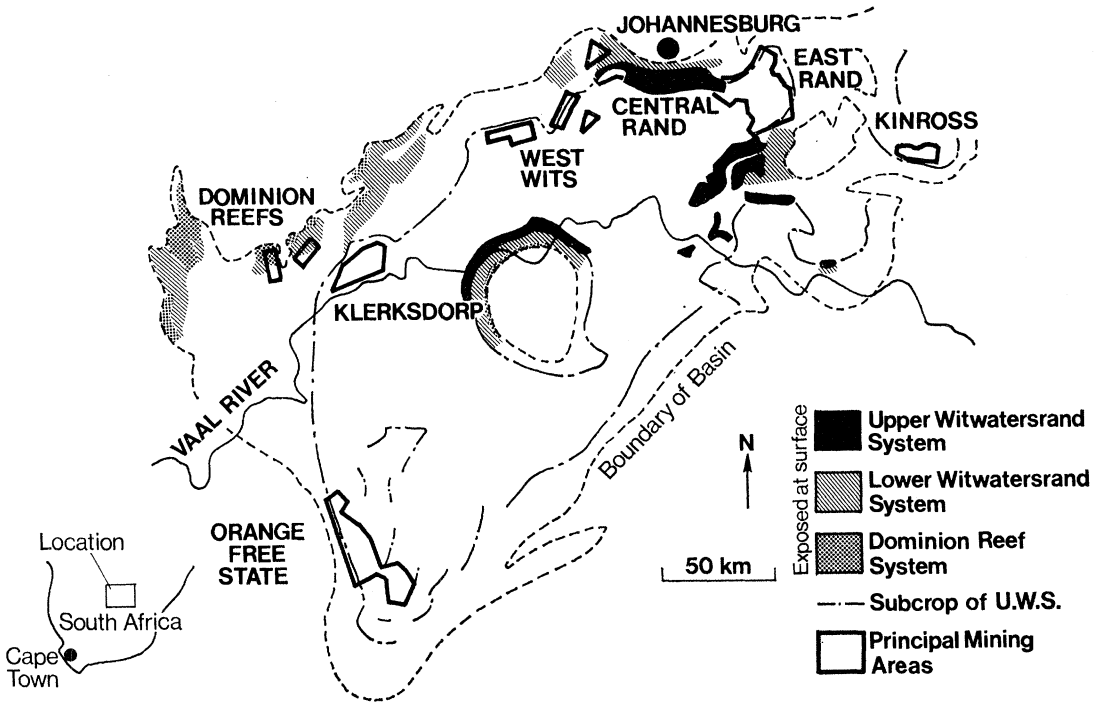

FIGURE 1. Map of the Witwatersrand Basin illustrating sub-Ventersdorp geology and showing principal mining areas.

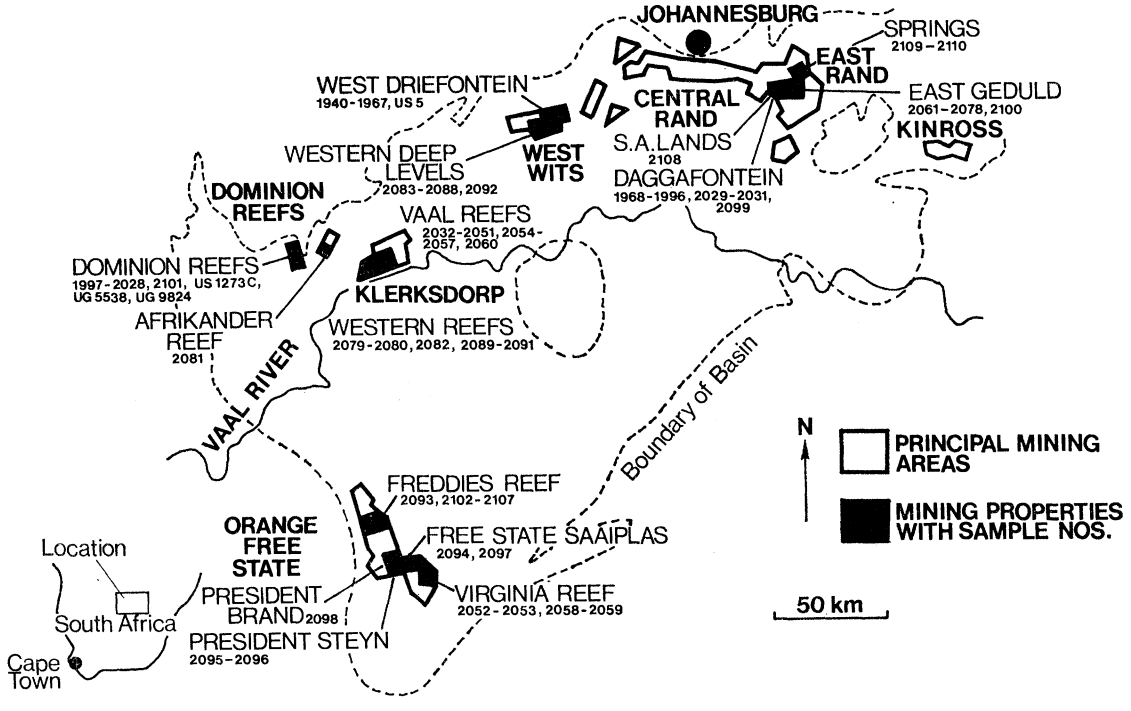

FIGURE 2. Map of the Witwatersrand Basin illustrating principal mining areas and sample localities. The numbers in small print refer to polished thin sections. Polished sections from the reference collection are prefixed (UG, US).

Experimental methods

The details of the complex mineralization and the distribution of uranium were elucidated by ore microscopy, electron probe microanalysis and fission track registration. The techniques of the first have been recently described by Bowie, Simpson & Atkin (1975) and the last is discussed below in the section on uranium micromapping.

The electron probe analyses were undertaken with a Cambridge Microscan-5 instrument fitted with a Canberra energy dispersive analytical system. The latter was used for the analysis of Ti, Mn, Fe, Pb, Th, U and Y, whilst Ca and Ce were analysed simultaneously by the Bragg spectrometers of the microprobe. X-rays from each specimen were counted for 250 s at a low beam current of 1×10^{-9} A, which conditions were suitable for both analytical systems. Data were reduced by a PDP11 computer, which calculates concentrations of the elements present at one analytical point while the next is being analysed. This technique enables an analysis for nine elements to be produced every 4 to 5 min. Pure metals were used as standards for Mn, Fe, Th and U, a rare-earth glass REE-3, kindly provided by the University of Oregon (Drake & Weill 1972) for Ca, Y and Ce, and chemically analysed rutile and galena for Ti and Pb respectively. The analytical methods for wavelength-dispersive analysis described by Bowles (1975) were used for Ca and Ce. In another paper, Bowles (in preparation) describes the quantitative analytical programme for the energy-dispersive equipment and compares selected results with those obtained with the Bragg spectrometers. The results are closely comparable for all elements with the exception of uranium for which the energy-dispersive results are consistently 3 % lower than the Bragg spectrometer results. Investigation has shown that as between the pure metal and the oxide there is a change in the ratio of the $L\alpha_1$ to $L\alpha_2$ intensities. The lower resolution of the energy-dispersive equipment records both X-ray emissions as a single peak, so that a variation in the ratio does not affect the results. The analyses presented here for uranium and thorium are those obtained using the energy-dispersive equipment. The measured concentrations were corrected using the quantitative correction programme devised by Mason, Frost & Reed (1969).

Mineralogical evidence

Pyrite

Pyrite is the principal opaque mineral of the Witwatersrand and Dominion Reef Systems. In hand specimen rounded grains of pyrite, commonly known as 'buckshot' (Feather & Koen 1975), display clearly defined sedimentary features with well-developed bedding and cross-bedding in layers also containing sand-sized grains of quartz. In the pebble-size conglomerate, pyrite occurs as a discrete disseminated phase together with other sand-sized constituents, principally quartz, in the matrix. Radioactivity is closely associated with pyritic zones in the hand specimen and those were therefore selected for more detailed investigation. Indeed, the presence of pyrite in the hand specimen is one of the clearest indications of the likely presence of anomalous radioactivity in the suite of specimens studied.

Ramdohr (1958), Saager (1970) and Köppel & Saager (1974), distinguished three types of pyrite in the Witwatersrand ore: I, allogenic; II, concretionary authigenic; and III, reconstituted authigenic. Type I pyrite has rounded and abraded outlines; it is completely fresh, is uniformly compact and homogeneous, and has a distinctive range of inclusions (figure 3*a*,

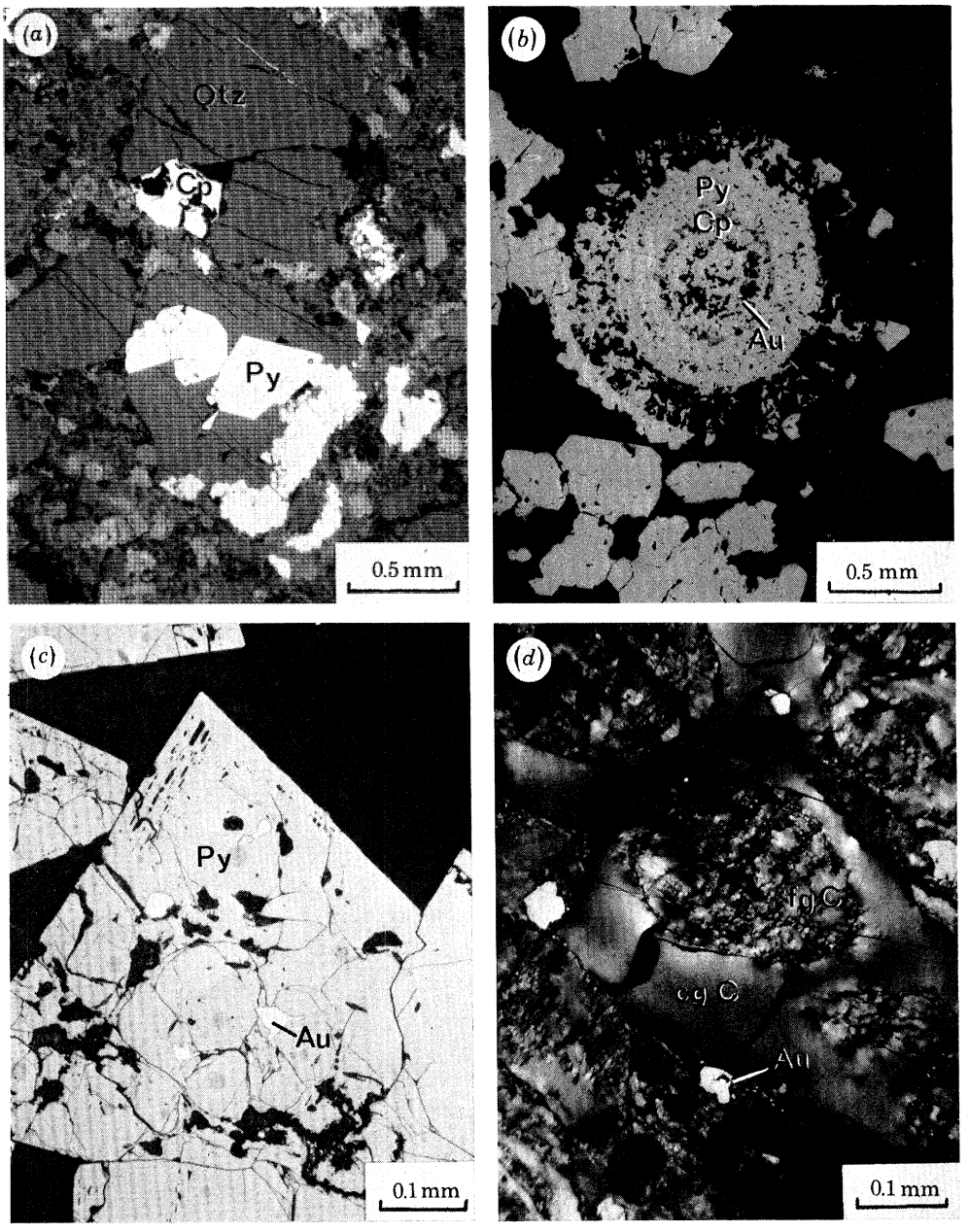

FIGURE 3 (*a*) Banket ore sample showing allogenic pyrite (Py), chalcopyrite (Cp) and quartz (Qtz); Dominion Reef, (US1273C), reflected light, air.

(*b*) Concretionary pyrite of spherical type composed of alternate layers of pyrite (Py) and chalcopyrite (Cp) with a grain of gold (Au). Silicates occur in the body of the concretion and particularly in the rim, as well as in the porous matrix (black). West Driefontein, West Wits (PTS 1966), reflected light, oil.

(*c*) Authigenic reconstituted pyrite (Py) containing gold (Au). West Driefontein, West Wits, (PTS 1958), reflected light, oil.

(*d*) Carbonaceous matter showing coarse (cgC) and fine-grained (fgC) carbon, with gold (Au). Carbon Leader, West Wits (US 5), reflected light, oil.

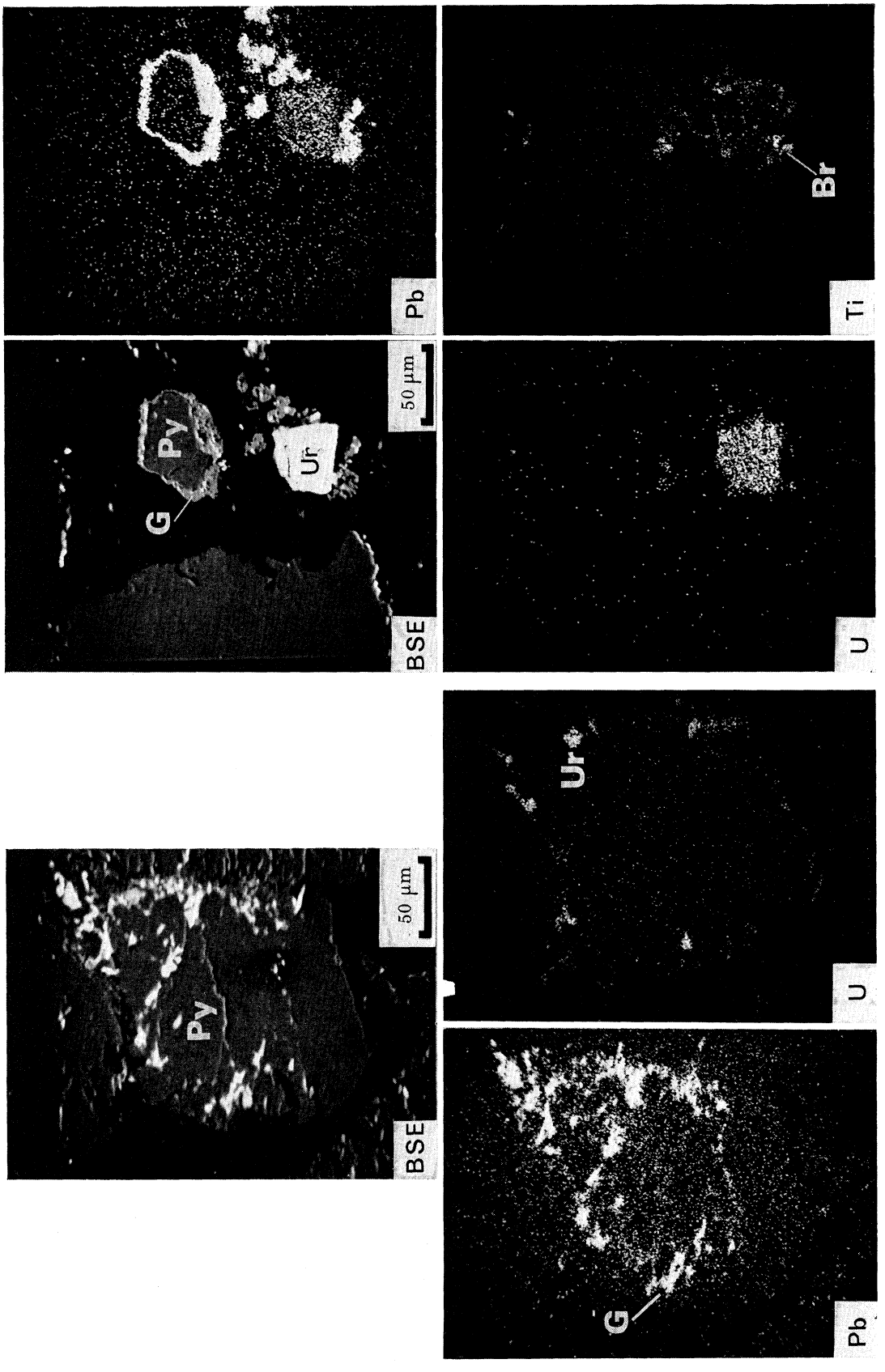

FIGURES 4 AND 5. For description see opposite.

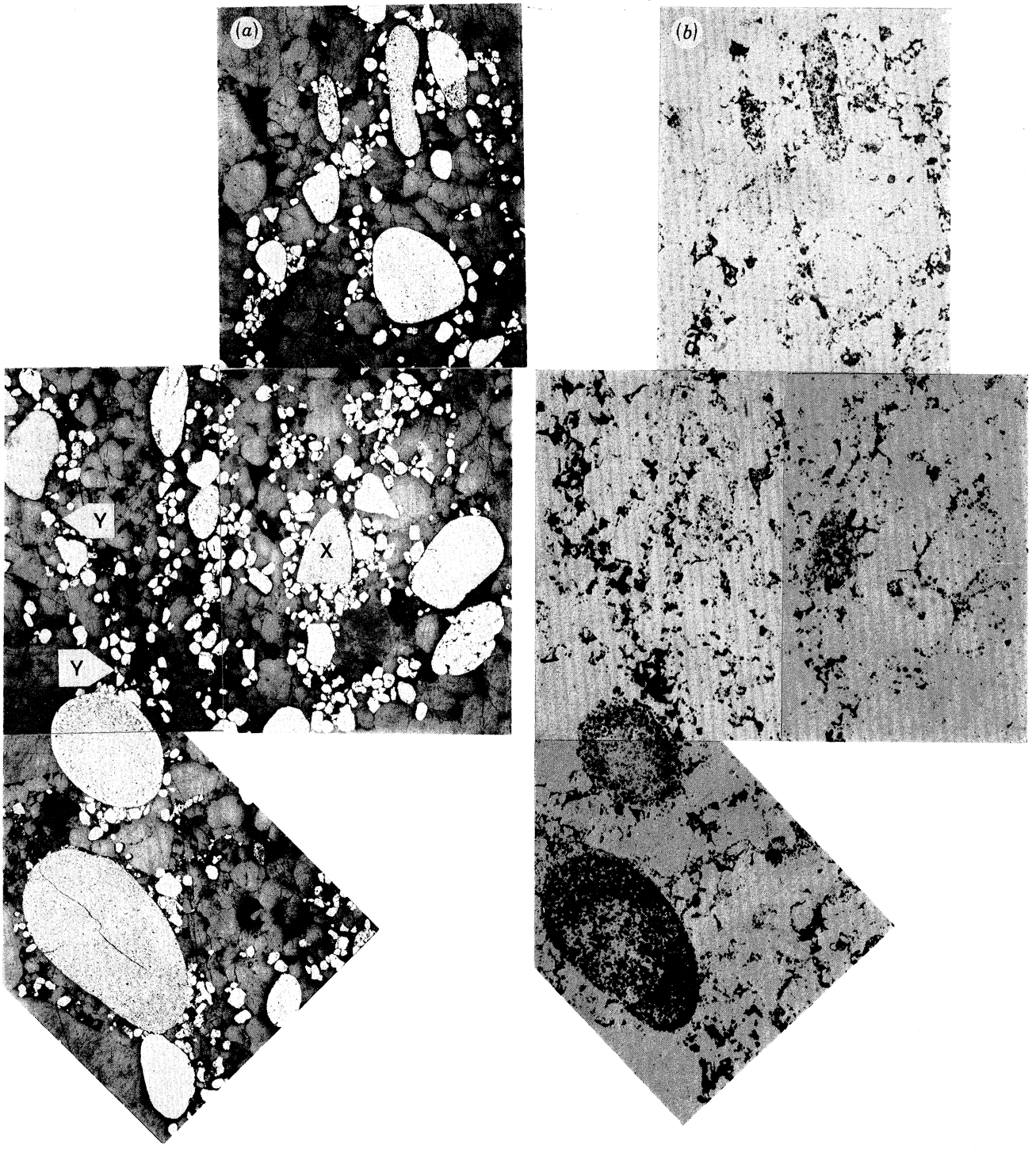

FIGURE 6. (*a*) Reflected light and (*b*) corresponding Lexan print showing a uraniferous pyritic band consisting of larger concretionary and smaller allogenic pyrite (white). Uranium is enriched in some concretionary pyrite grains but not in others (see Lexan print). One concretionary pyrite grain (*X*) has been fractured and further worn before deposition. Uranium present in the matrix is accounted for by allogenic grains of uraninite (*Y*), and interstitial clay minerals; Basal Reef, President Brand, Orange Free State (PTS 2463B).

FIGURE 4. Electron probe scanning images showing allogenic pyrite (Py) containing galena (G) and rimmed by uraninite (Ur); Basal Reef, President Brand, Orange Free State (PTS 2463A).

FIGURE 5. Electron probe scanning images showing localized migration of radiogenic lead from uraninite (Ur) to the rim of an adjacent allogenic pyrite (Py) grain with formations of minor amounts of brannerite (Br); Basal Reef, President Brand, Orange Free State (PTS 2463A).

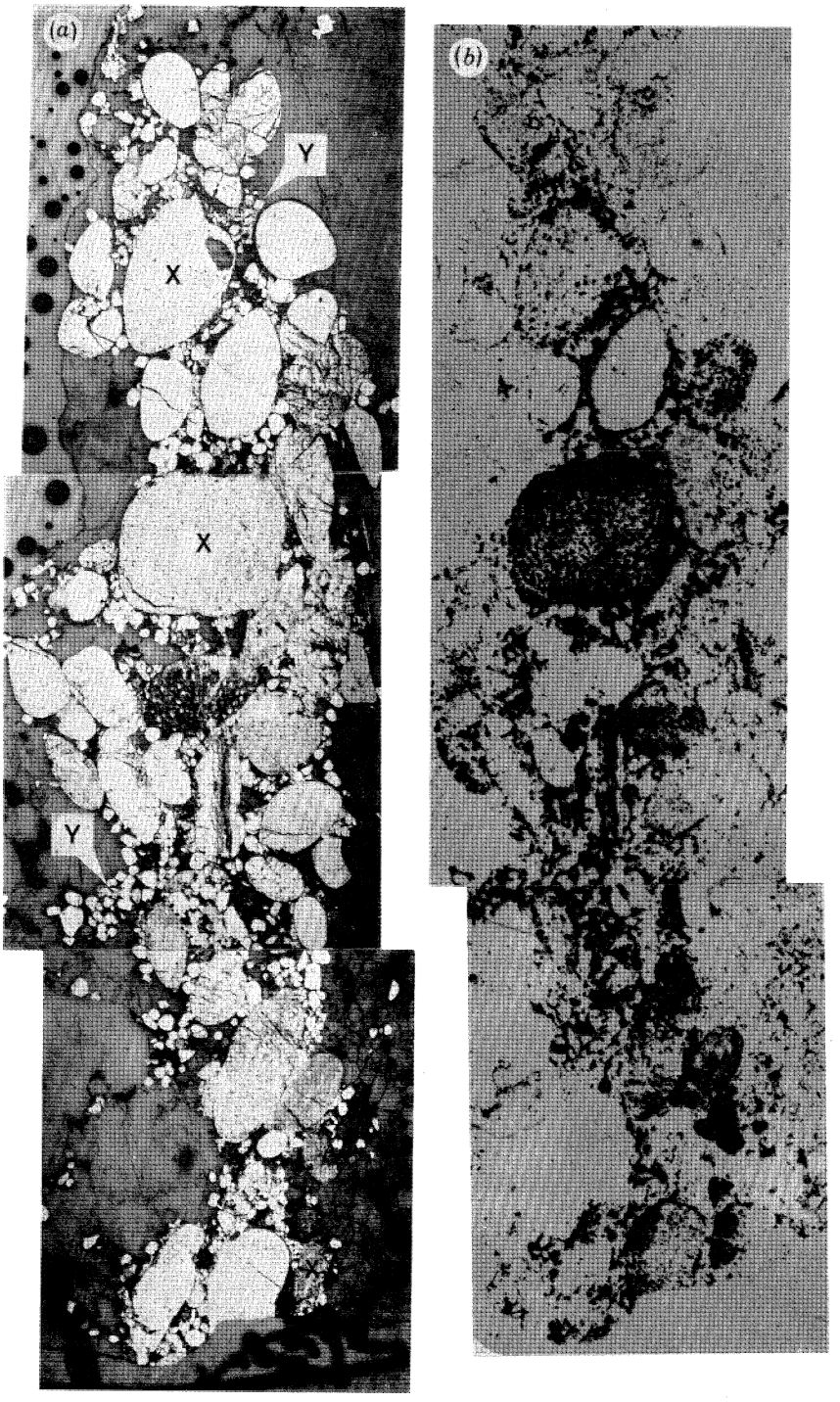

FIGURE 7. (*a*) Reflected light and (*b*) corresponding Lexan print showing uraniferous pyrite band consisting of mainly concretionary pyrite grains (white) which are a heterogeneous assemblage with regard to uranium enrichment (see Lexan print and compare grains marked *X*). Uranium present in the matrix is accounted for by the presence of allogenic grains of uraninite (*Y*) and interstitial clay minerals; Basal Reef, President Brand, Orange Free State (PTS 2463A).

plate 1). There is no doubt it is correctly described as allogenic. It is recognized in this study as the dominant pyrite type of the Dominion Reef System, whereas in the Witwatersrand any one of the three types may be dominant. Pyrite of this type also occurs partially or completely enclosed within very coarse quartz grains; it displays euhedral grain boundaries towards the host quartz, but has a sub-rounded and abraded margin where it forms the exterior of the composite grain (figure 3*a*). Optical study and electron probe microanalysis indicate that galena is the commonest phase included in allogenic pyrite. The exsolution blebs of galena (figure 4, plate 2) are distinct from marginal intergrowths of pyrite and galena resulting from the migration of radiogenic lead from coexisting uraninite grains (figure 5, plate 2).

Pyrite of type II is present in variable amounts in all samples studied from the Witwatersrand System. It is readily distinguished from type I by its porous nature and from type III by its rounded outline. The concretions are generally coarser than coexisting allogenic pyrite, ranging from granular to coarse sand size, although the individual pyrite crystallites that form the concretions are often 10 μm in diameter or less. However, in any one specimen the concretions are heterogeneous in nature with regard to shape, size and crystallite composition. Some concretions have spherically zoned alternating sulphide and silicate shells, others exhibit a layered structure. Some are so dark and fine-grained as to be indistinguishable from melnikovite or colloform pyrite, which is thought to represent a crystallized FeS_2 gel.

In the concretionary pyrite, the coarser crystallites, which are better crystallized and brighter, are texturally very similar to framboidal pyrite. The pore spaces between crystallites represent about 10% by volume of the concretions, although zones occur where the pyrite content may be as low as 10%. Even within one concretion the texture may be very variable, ranging from fine-grained disseminated pyrite to a more compact equigranular variety without pore spaces between crystallites. Saager & Mihálik (1967) proposed that these concretions formed *in situ* since they claimed the 'extremely delicate nature of the concretions exclude any long transport distance'. However, it should be noted that the crystallites forming the concretions are in most cases interconnecting, thereby providing a rigid skeleton, and the pore spaces between crystallites are filled by a matrix comprising quartz and a 7 Å clay mineral (unidentified) which provides additional strength to the concretions. Most of these composite structures have survived later metamorphism and deformation relatively unaltered. Moreover, coexisting detrital quartz granules show appreciable pressure solution effects along their margins, though both allogenic and concretionary grains occurring in close proximity are undeformed, testifying to their relative rigidity and strength.

In our view the heterogeneity of the concretionary pyrite in any hand specimen and the evidence of some rounded granules that have apparently been fractured and abraded before deposition, indicate that most of the concretionary pyrite has been transported to its present location and did not form *in situ* (figure 6, plate 3). The variability of this pyrite in any particular sample is considered to reflect a source area and selective effects of transportation processes. The intimately intergrown nature of the sulphide and silicate phases in the concretions is most probably a primary feature inherited from the source area and is not due to subsequent introduction of silica, since the regular fine-scale laminations observed in some cases preclude the possibility of later introduction (figure 7, plate 4). Hallbauer (1975) has described sub-spherical concretions of this type extracted for study by scanning electron microscopy as 'pyritized mudballs' and this would appear to be a satisfactory, yet simple, genetic description accounting for much of the concretionary pyrite studied here. However, there are rare

occurrences of zoned spherical concretions. The example shown (figure 3*b*) has a thin inner zone of chalcopyrite with rare grains of gold, and a siliceous rim partially overgrown by pyrite. The spherical outline is clearly a primary feature and deductions about the extent to which transport may or may not have occurred, cannot in general, be made from a study of external form alone.

Electron probe scans of the concretionary pyrite in one specimen, 2463A, indicate that the lead content, represented by galena, varies widely in amount and distribution from concretion to concretion. In some (figure 8, plate 5) galena is rare. Others have a high content of disseminated galena in 10 μm grains uniformly distributed throughout the concretion (figure 9); and some have fine veinlets of galena probably representing later introduction of lead.

Pyrite of type III occurs as euhedral grains in the conglomerate matrix or forms overgrowths on detrital components. It is clearly authigenic in origin. Köppel & Saager (1974) report enrichments of chalcopyrite, sphalerite and galena associated with the development of this pyrite type and also remark that the presence of dykes instrusive into the Witwatersrand rocks has influenced its development. However, these authors attribute the bulk of this reconstituted pyrite to regional metamorphism. The presence of grains of gold, in some cases abundant, noted in pyrite of this type during the present study (figure 3*c*), indicates that gold and pyrite were locally remobilized and redeposited together.

Uraninite

Before describing the details concerning the analysed material, it is necessary to comment on the use of the terms uraninite and pitchblende. Uraninite is the name for the species as a whole including all of its varieties (Frondel 1958). Pitchblende is a variety of uraninite distinguished primarily by its appearance. In the Witwatersrand all detailed work to date shows that uraninite found there can be divided into two groups. A well-crystallized variety with significant thorium content, and a poorly crystallized variety which only occurs in association with organic matter and has a low thorium content. As these tend to be found in different environments it is important to distinguish between them, so in this paper 'uraninite' is restricted to the well crystallized variety and 'pitchblende' to the other.

Uraninite occurs as discrete allogenic grains varying in shape from euhedral to subrounded and rounded grains, usually within a limited size range in the fine to very fine sand sizes (0.06–0.25 mm) and is often fractured. It occurs in this form both in the Dominion Reef and Witwatersrand Systems. Thorium content is the best indicator of primary differences in populations of uraninite grains since lead content within and between grains may be quite variable due to exsolution and migration of radiogenic lead. This lead mobility has a greater effect on the uranium content than on thorium which has a more homogeneous distribution, and is less readily displaced. It is possible to observe in some cases the migration and reaction of radiogenic

---

DESCRIPTION OF PLATE 5

FIGURE 8. Electron probe scanning images showing a discrete galena (G) grain occurring in a low-lead type pyrite concretion (Py). Uranium is present in the interstitial clay phase (*c*). Compare with figure 9 showing lead distribution in a pyrite concretion from the same section Basal Reef, President Brand, Orange Free State (PTS 2463A).

FIGURE 9. Electron probe scanning images showing galena distribution (G) in concretionary pyrite of high-lead type. Compare with low-lead type in figure 8. Basal Reef, President Brand, Orange Free State (PTS 2463A).

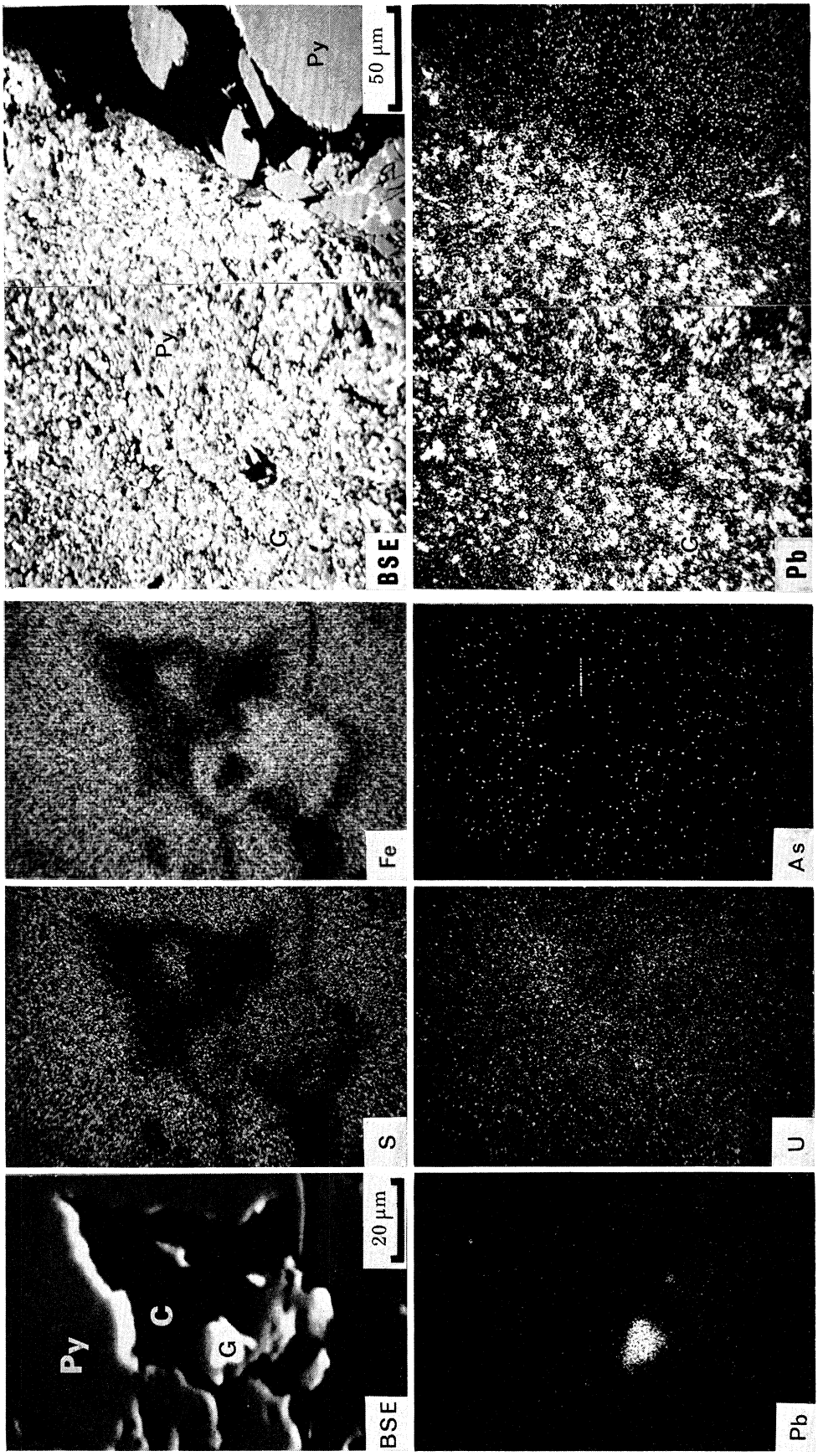

FIGURES 8 AND 9. For description see opposite.

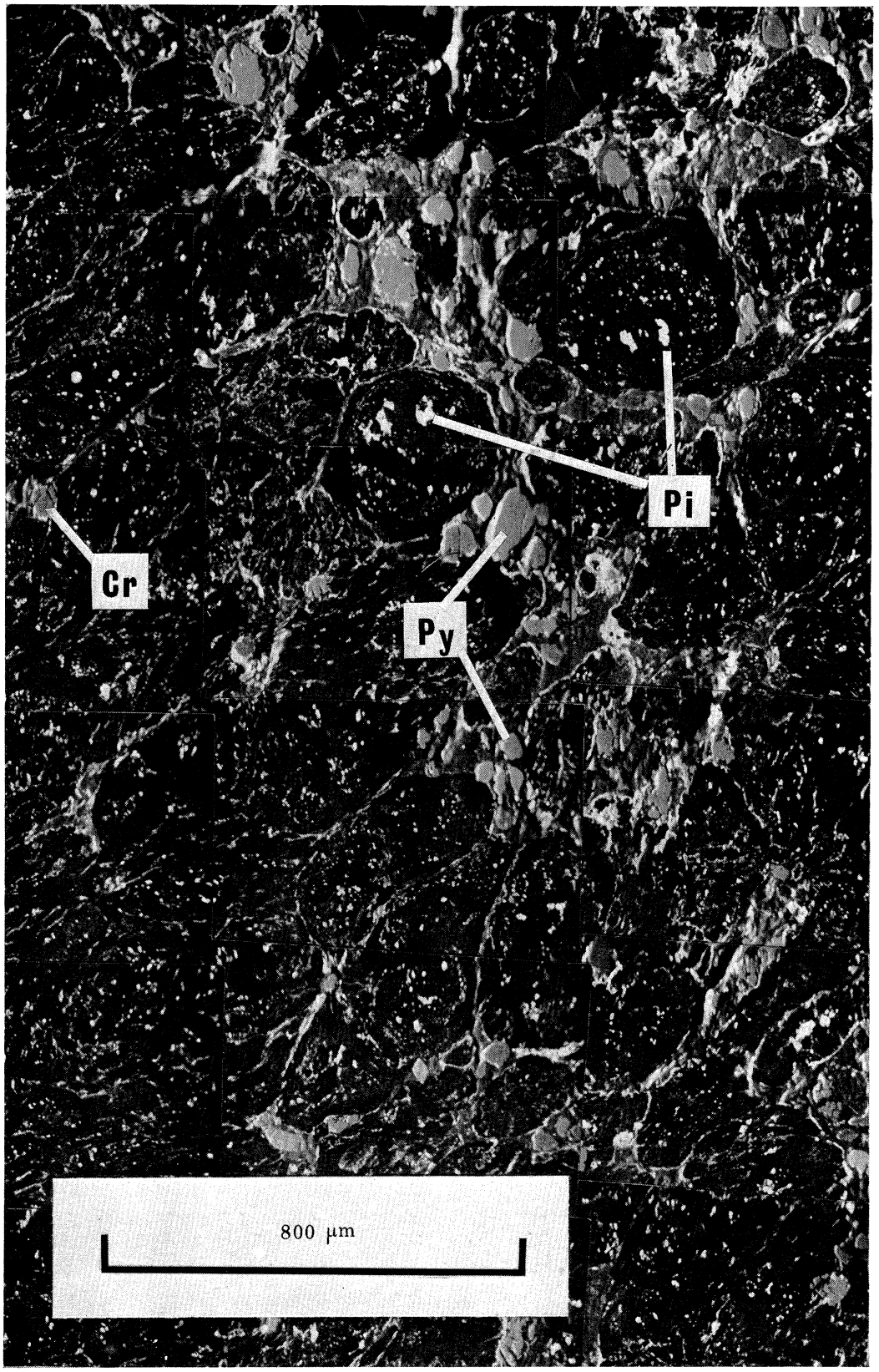

FIGURE 13. Electron probe backscattered electron image of granular carbonaceous material containing fine-grained particles of pitchblende (Pi) and gold in a carbonaceous matrix (black). Allogenic grains of pyrite (Py) and chromite (Cr) occur interstitially to the granular carbon but allogenic uraninite was not detected; Carbon Leader, West Wits (US 5).

lead with nearby allogenic sulphide to form a galena rim (figure 5). In the same section the close proximity of brannerite to decaying uraninite, with non-uraniferous titanium minerals at a greater distance is indicative of local migration and reaction of uranium with titanium minerals in the sediments.

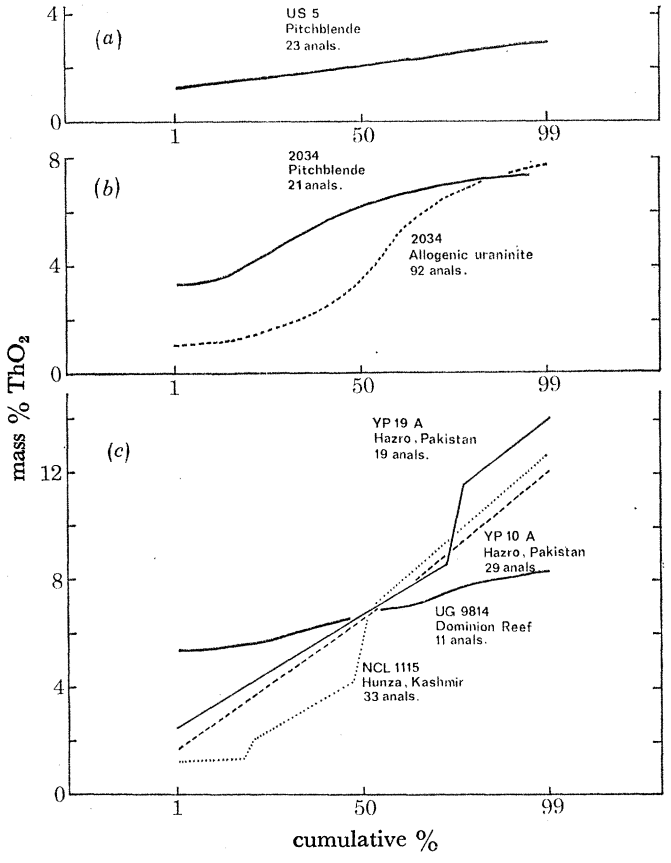

FIGURE 10. Cumulative frequency diagrams for ThO_2 obtained by electron probe microanalysis:

(*a*) Mass % ThO_2 of fine pitchblende grains in granular 'flyspeck' carbon, Carbon Leader, West Wits, (US 5).

(*b*) Mass % ThO_2 of coexisting granular allogenic uraninite and fine-grained pitchblende in columnar carbon, Vaal reefs, Klerksdorp (PTS 2034).

(*c*) Mass % ThO_2 of allogenic uraninite for one sample from the Hunza river, Kashmir a tributary of the Indus, two samples from Hazro, Pakistan on the Indus and one sample from the Dominion Reef.

Electron microprobe analyses show in this study that the Dominion Reef uraninite has a median ThO_2 content of 6.6 % with a range from 5.4 % to 8.4 % (figure 10*c*) and a median UO_2/ThO_2 ratio of 8.5 with a range from 6.4 to 10.9 (figure 11).

In the Vaal Reef of the Witwatersrand System, allogenic uraninite analysed in a columnar carbonaceous band (PTS 2034) has a median ThO_2 content of 3.5 % with a range from 0.9 to 9.1 % (figure 10*b*) and a median UO_2/ThO_2 ratio of 19 with a range of 8.3 to 48 (figure 11). The separate populations of ThO_2 in uraninite grains from the Dominion and Vaal Reefs were tested by analysis of variance methods and found to be significantly different at the 0.001 level, but variations within these populations are not significant. Significant positive correlation between calcium and manganese, and between iron and manganese is common to both uraninite populations.

The ThO_2 content, UO_2/ThO_2 ratio and correlation between calcium and manganese and iron and manganese probably reflect conditions of crystallization in the source area. The higher median UO_2/ThO_2 ratios for the Vaal reef uraninite and the lower Th content compared with uraninite from the Dominion Reef, indicates some variation in the source area for the two horizons. However, fluid-inclusion studies do not reveal any differences in the quartz pebbles (Shepherd, this volume).

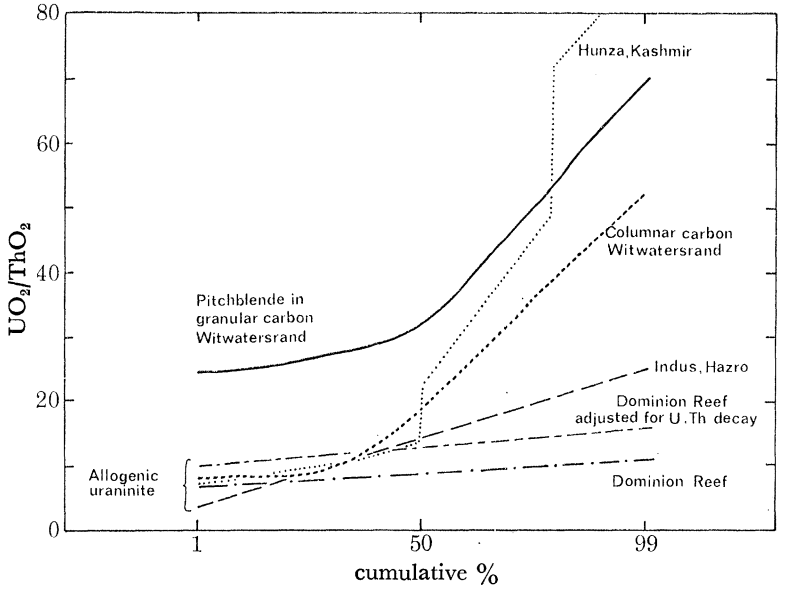

FIGURE 11. UO_2/ThO_2 ratios for separate populations of uraninite and pitchblende plotted on a cumulative frequency diagram. The highest median values are given by fine-grained pitchblende in granular carbon from the Carbon Leader (US 5). Allogenic uraninite from the Vaal reefs in the Witwatersrand (PTS 2034) has a lower ratio which is still higher than uraninite from the Dominion Reef (UG 9824). Detrital uraninite from the Indus river at Hazro (YP 10A and YP 19A) and the Hunza river, Kashmir, a tributary of the Indus, is plotted here for comparison with the Dominion Reef and Witwatersrand samples as they occur at present time. The Dominion Reef samples have also been recalculated to take account of decay of U and Th since crystallization at ~ 3000 Ma, and this correction tends to reduce the small difference between populations.

Grain size of uraninite and associated phases

A typical sample (UG 5538) from the Bramley section of the Dominion Reef mine, Klerksdorp, was examined in detail by grain-size analysis. Coexisting allogenic grains of quartz, pyrite, uraninite and gold were measured by means of the Humphries eyepiece micrometer, which can be used to classify grains directly according to the phi scale. Each population, except for gold, consisted of a hundred grains measured along the Feret diameter, which is the maximum grain length projected on to a fixed line. The populations appear to be single populations in each case resulting in linear cumulative frequency curves. Sample means and standard deviations were calculated in terms of phi units from which the standard error of the mean was obtained. This was transferred to a chart containing graphical results calculated for Stokes law and the square-root law combined (Tourtelot 1968), which indicates that quartz, pyrite and uraninite closely approximate to a hydraulically equivalent assemblage (figure 12). The gold grains counted were too few to be statistically significant, but nevertheless appear too small for exact hydraulic equivalence. This point was noted by Coetzee (1965), but no satisfactory explanation has yet been proposed.

Uraniferous and auriferous carbonaceous material

Uranium and gold in association with carbonaceous material is one of the most important modes of occurrence of these metals in the Witwatersrand Basin, particularly in view of the uniformly high grades of mineralization encountered and the wide lateral extent of such horizons as the Carbon Leader in the Far West Rand (Davidson & Bowie 1951; Bourret 1973).

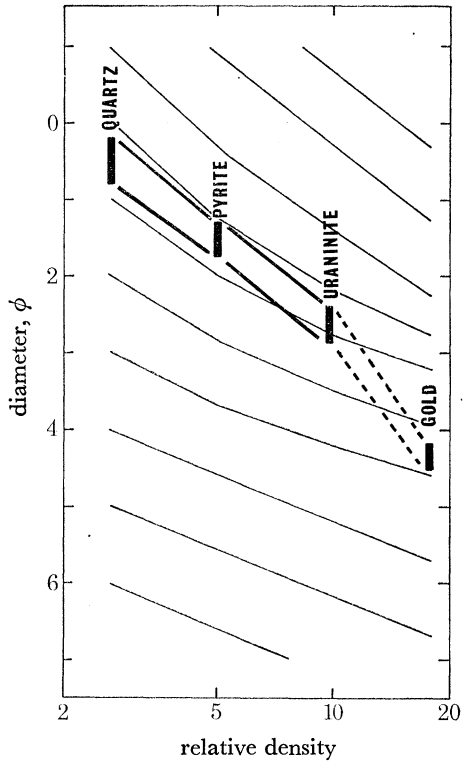

FIGURE 12. Standard error of the mean size for coexisting quartz, pyrite and uraninite plotted on the phi scale against specific gravity. The light curves are solutions for Stokes' law and the square-root law combined where they overlap. The relative grain sizes of the suite of minerals plotted in heavy type indicate that quartz, pyrite and uraninite are hydraulically equivalent. The gold is smaller than would be expected for hydraulic equivalence but the number of grains measured is inadequate for full statistical treatment, Bramley high grade, Dominion Reef (UG 5538), diagram after Tourtelot (1968).

Any satisfactory explanation of the nature of this metal-rich carbonaceous matter should take account of the following observations: (*a*) The Carbon Leader, which represents a most striking enrichment of uranium and gold, forms a very restricted horizon in the reef never greater than 13 mm thick (Davidson & Bowie 1951). (*b*) The consistently high levels of both uranium and gold over a wide lateral extent. (*c*) The higher UO_2/ThO_2 ratios in the carbonaceous type of mineralization compared with the banket type of both the Witwatersrand and Dominion Reef Systems, and its absence in the latter; (*d*) The absence of mineralization in certain occurrences of carbonaceous material. Some authorities consider the carbonaceous material represents fossilized remains of Precambrian plants (Hallbauer 1975). Whether such is its origin or not, there is little doubt that it has exercised a key rôle in the formation of these deposits.

The carbonaceous material comprises granular and columnar varieties, which have many features in common whilst differing in certain important aspects (Davidson & Bowie 1951). According to the analyses of Davidson & Bowie this material contains 43 % C and 2 % H and they called this phase hydrocarbon. However, we have not attempted to define the organic constituents of all the carbonaceous materials studied here and have therefore retained a more general nomenclature used by Vine *et al.* (1958).

The granular or 'fly speck' material (figure 13, plate 6) consists of ovoid to rounded grains (100–400 μm) with an interstitial matrix of sub-rounded allogenic pyrite, chromite and concretionary pyrite ($\sim$ 50 μm). The granules are partially moulded around interstitial grains, particularly where they lie along grain boundaries between granules (figure 13), but the carbonaceous matter at no point either replaces or invades the opaque minerals. The granules have mottled extinction under crossed polars in reflected light and contain two main phases of carbonaceous matter (figure 3*d*), consisting of relatively coarse-grained smooth areas with undulose extinction interspersed with fine-grained material having a similar reflectance of 14.3 % (Type (I) of Davidson & Bowie 1951, p. 6). The fine-grained material is veined along grain boundaries by a dendritic system containing pitchblende, gold, pyrite, galena and gersdorffite. The gold and gersdorffite are commonly intergrown, as are the gold and pitchblende. Galena tends to form separate grains, but is also intergrown with pyrite. These textural and mineralogical relationships have been confirmed by both scanning and quantitative electron probe analysis. The pitchblende has a median ThO_2 content of 2.0 % with a range from 1.1 to 2.9 % (figure 10*a*) and a median UO_2/ThO_2 ratio of 33 with a range from 25 to 69 (figure 11). Analysis of variance shows that this population is significantly lower in its ThO_2 content at the 0.001 level than all the other uraninite and pitchblende phases in the Witwatersrand and Dominion Reef. There is significant correlation between uranium and calcium (0.01 level) uranium and cerium (0.01 level), and PbO and ThO_2 (0.001 level). However, there is no correlation between calcium and manganese or between iron and manganese as for the allogenic uraninite, pointing to a distinct origin for the pitchblende in the granular carbon, which probably developed *in situ* during diagenesis and metamorphism.

The carbonaceous seam of the Carbon Leader usually occurs along the basal parting in quartz pebble conglomerate, and has a well-developed columnar structure normal to the bedding. It is linked with, but different from, the granular form described above. It consists of the same two carbon phases, occurring as lenticular to ovoid bodies with their long axes normal to the bedding. Individual bodies are cut by discontinuous vertical sutures which emphasize the overall columnar effect (figure 14, plate 7). Scanning electron-probe studies demonstrate that these sutures carry fine-grained pitchblende, brannerite, gold and other phases (figure 15, plate 7).

The inclusions within the columnar carbonaceous material are similar mineralogically to those in the granular material with one notable exception, namely the occurrence of coarse-grained uraninite, often subrounded and partly replaced by coarse-grained carbonaceous matter (figure 16, plate 8). This uraninite is concentrated along one margin of the carbon seam though not restricted to that margin. Analyses of neighbouring fragments show that they belong to groups within which the ThO_2 content is similar, but may differ very considerably from that in adjacent groups, indicating a chemically heterogeneous assemblage of uraninite crystals subsequently fragmented and replaced by carbonaceous matter (figure 17, plate 8). The chemistry of the allogenic uraninite grains has been described above and is shown in

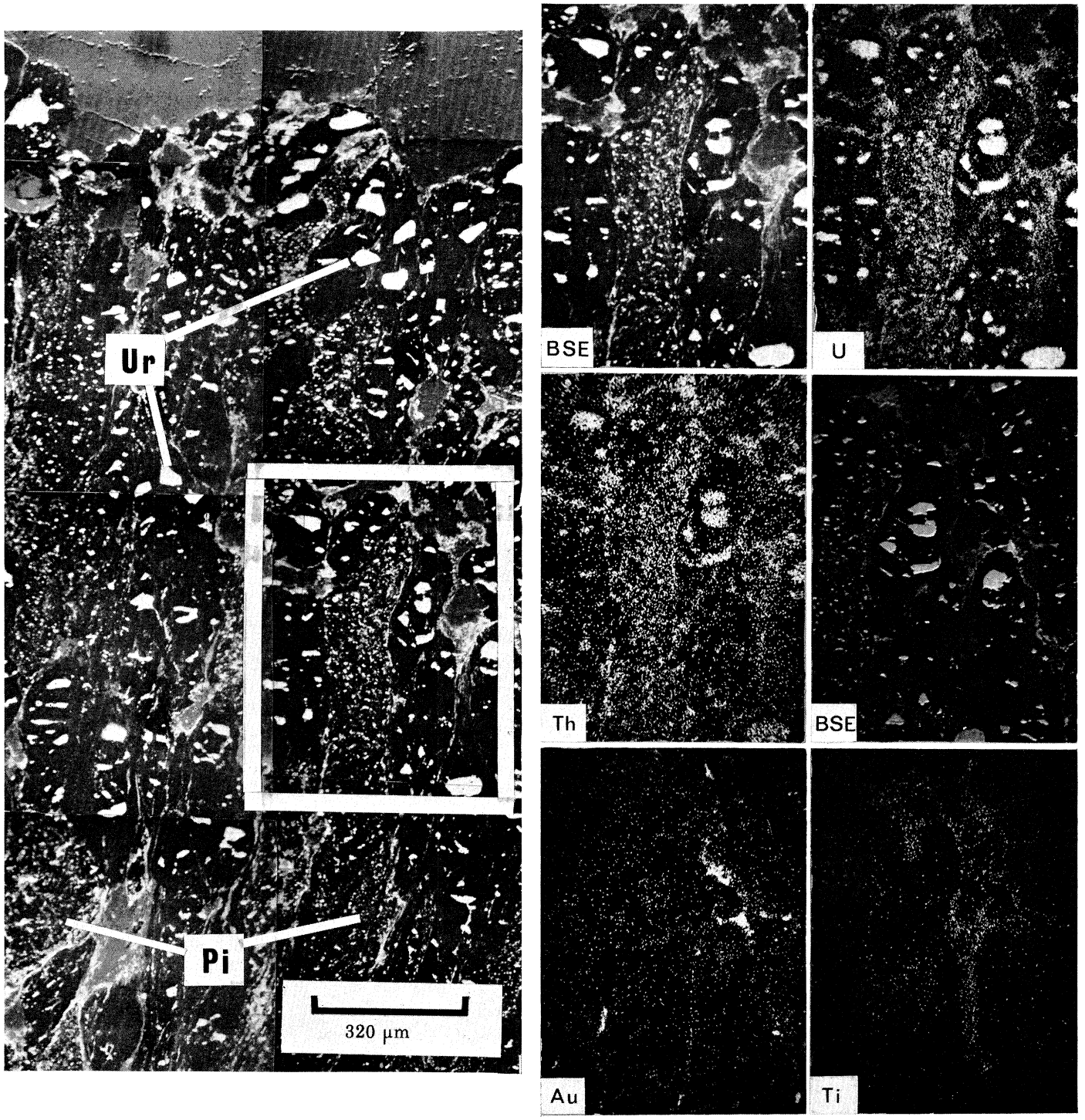

FIGURE 14. Electron-probe backscattered electron image of columnar carbon showing zones of coarse fragmented allogenic uraninite (Ur) and fine-grained disseminated pitchblende in a carbonaceous matrix (black). Vertical lineations of a strongly reflecting phase between these zones consist of fine disseminations of gold associated with brannerite, pitchblende and churchite; Vaal Reefs, Klerksdorp (PTS 2034).

FIGURE 15. Electron probe scanning images from two overlapping areas of columnar carbon within inset on figure 14 showing backscattered electron images and distribution of uranium and thorium corresponding to coarse-grained uraninite and fine-grained pitchblende. The latter is intimately associated with gold and a titaniferous phase, probably brannerite, in a carbonaceous matrix (black). Vaal Reefs, Klerksdorp (PTS 2034).

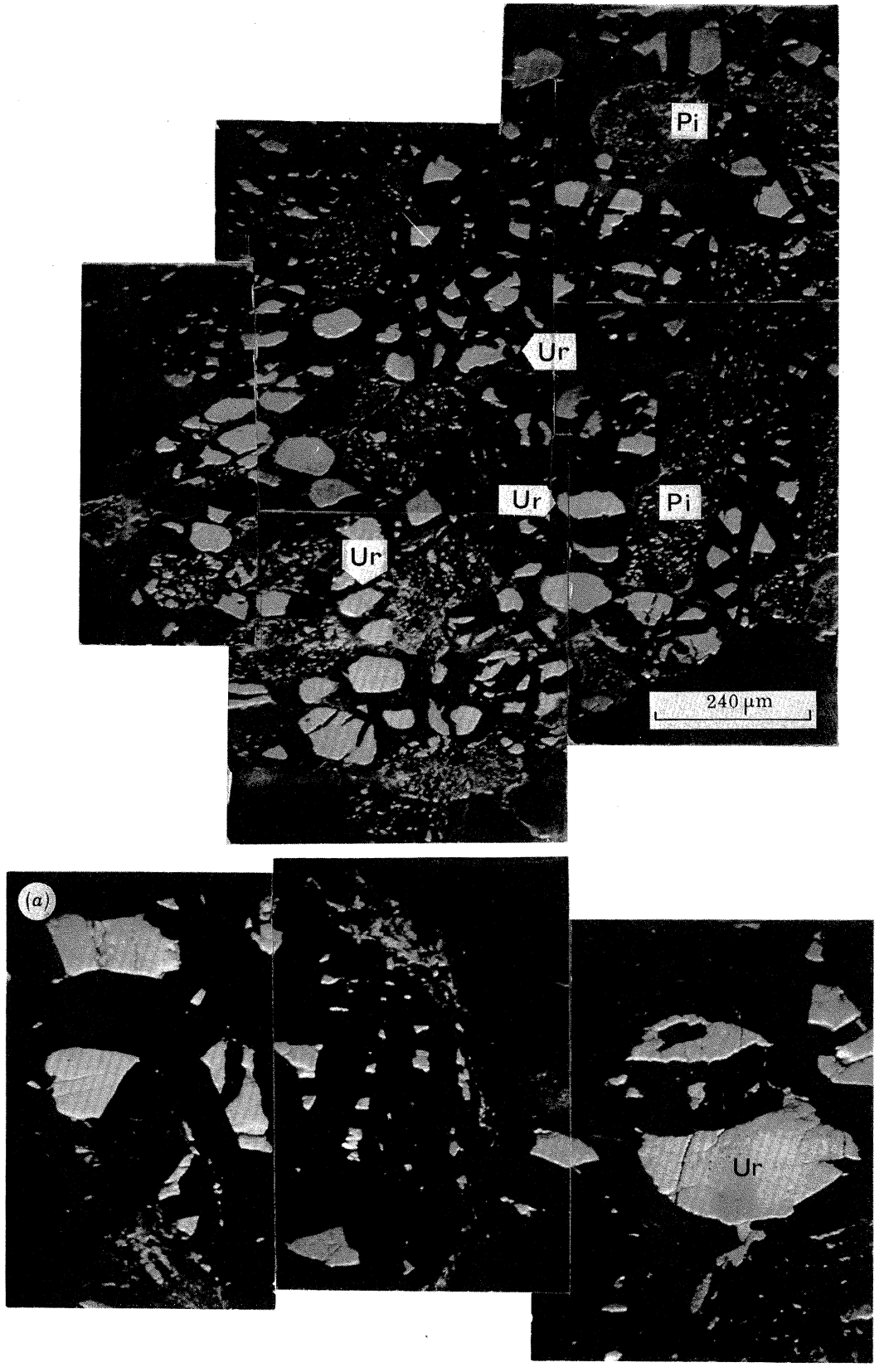

FIGURES 16 AND 17 (*a*). For description see opposite.

figures 10 and 11. Pitchblende, associated with partially replaced allogenic uraninite has a much higher thorium content than the pitchblende in the granular carbonaceous matter; it has a median ThO_2 content of 6.2 % with a range from 3.17 to 6.9 % (figure 10*b*) and a median UO_2/ThO_2 ratio of 9.0 with a range from 6.2 to 12.2. This population is significantly different from the coexisting coarse-grained allogenic uraninite (0.001 level), but not from the uraninite in the Dominion Reef. It is possible that the high thorium content is attributable to solution and redeposition of both uranium and thorium from the allogenic uraninite undergoing attack by carbonaceous matter.

The disseminated pitchblende in fine-grained columnar carbonaceous matter is optically and texturally very similar to that in the granular variety and is also intimately associated with galena, gersdorffite, gold and pyrite, forming an interconnecting dendritic texture of microcrystals in the manner previously described.

The outer margin of the carbonaceous matter, where it is in contact with allogenic pyrite, is a favoured site for gold concentration in the form of fine platelets. Internal pore spaces within carbonaceous matter are also an important site for the formation of complex intergrowths of uraniferous silicates, gold and gersdoffite. Partially replaced uraninite within carbonaceous material is also a common site for gold overgrowths. All these textures suggest that much of the

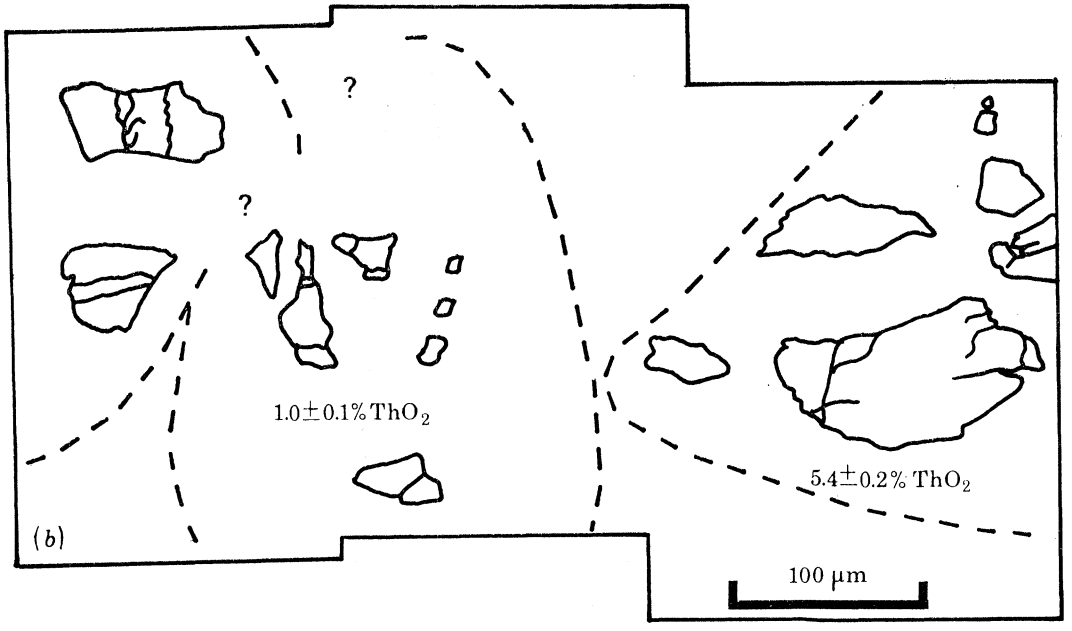

FIGURE 17(*b*).

DESCRIPTION OF PLATE 8

FIGURE 16. Electron probe backscattered electron image of columnar carbonaceous material showing clusters of coarse-grained allogenic uraninite crystals (Ur) partly digested by carbonaceous matter (black) with lobate zones of fine-grained pitchblende (Pi) in a carbonaceous matrix. Vaal Reefs, Klerksdorp (PTS 2034).

FIGURE 17. (*a*) Electron probe backscattered electron image showing uraninite within carbonaceous material. The destruction of large uraninite grains by the carbonaceous material is shown by the complementary outlines of adjacent grains and in the reconstruction of original grain outlines. (*b*) The ThO_2 content clearly demonstrates similarity within but differences between grains outlined, Vaal Reefs, Klerksdorp (PTS 2031).

gold, pitchblende, churchite (see below) and associated sulphides crystallized in their present position as a result of diagenetic or later metamorphic processes.

Churchite

A tenuous phase surrounds the fine-grained pitchblende of the columnar carbon (figure 18, plate 9). It contains major yttrium and phosphorous with the heavy rare-earth elements Gd, Tb, Dy, Er and Yb, corresponding to either xenotime (YPO_4) or churchite ($YPO_4.2H_2O$). Comparison of the rare-earth distribution (table 1) with that reported in the literature for xenotime and churchite points to an identity with the latter because of the distinct enrichment of the former in Dy, Er, and particularly Yb, relative to Gd.

This is particularly interesting in the present context, since xenotime is found principally in granitic pegmatites whereas churchite† can be formed by a combination of biochemical processes and diagenetic reactions close to the surface (Milton *et al.* 1944). In the occurrence des-

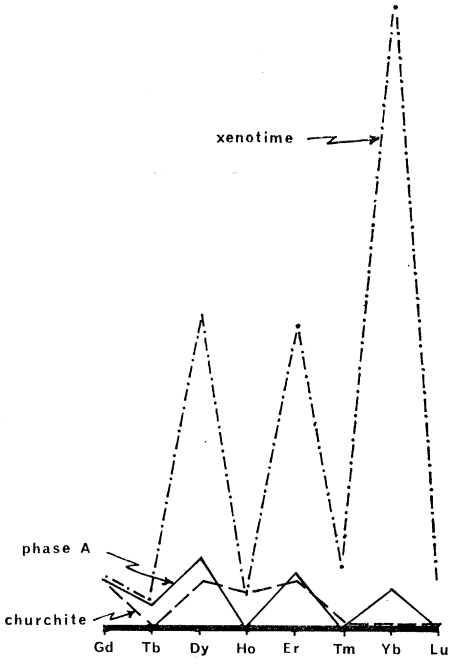

FIGURE 18*b*.

DESCRIPTION OF PLATE 9

FIGURE 18. (*a*) Electron probe scanning images of phase 'A' probably churchite, containing major Y and P which overgrows pitchblende (Pi). The example shown occurs in fibrous material within columnar carbon shown in figure 14. (*b*) The distribution of heavy rare-earth elements in phase A relative to gadolinium is compared here with examples of churchite and xenotime from the literature, Vaal Reefs, Klerksdorp (PTS 2034).

FIGURE 19 (*a*) and (*b*) Indus River uraninite.

(*a*) Uraninite grains from the Hunza river, Kashmir, a tributary of the Indus River. The uraninite grains usually show at least one crystalline face and several cubes are present. The grain shown in detail (*b*) exhibits alteration along discrete zones parallel to well-developed crystal faces. Most of the grains in the sample, however, are fresh and unaltered. No correlation between degree of alteration and ThO_2 content has been detected.

† Described as weinschenkite by Henrich (1935), Milton *et al.* (1944) and Pokrovskiy *et al.* (1965), but shown to be churchite by Claringbull & Hey (1953).

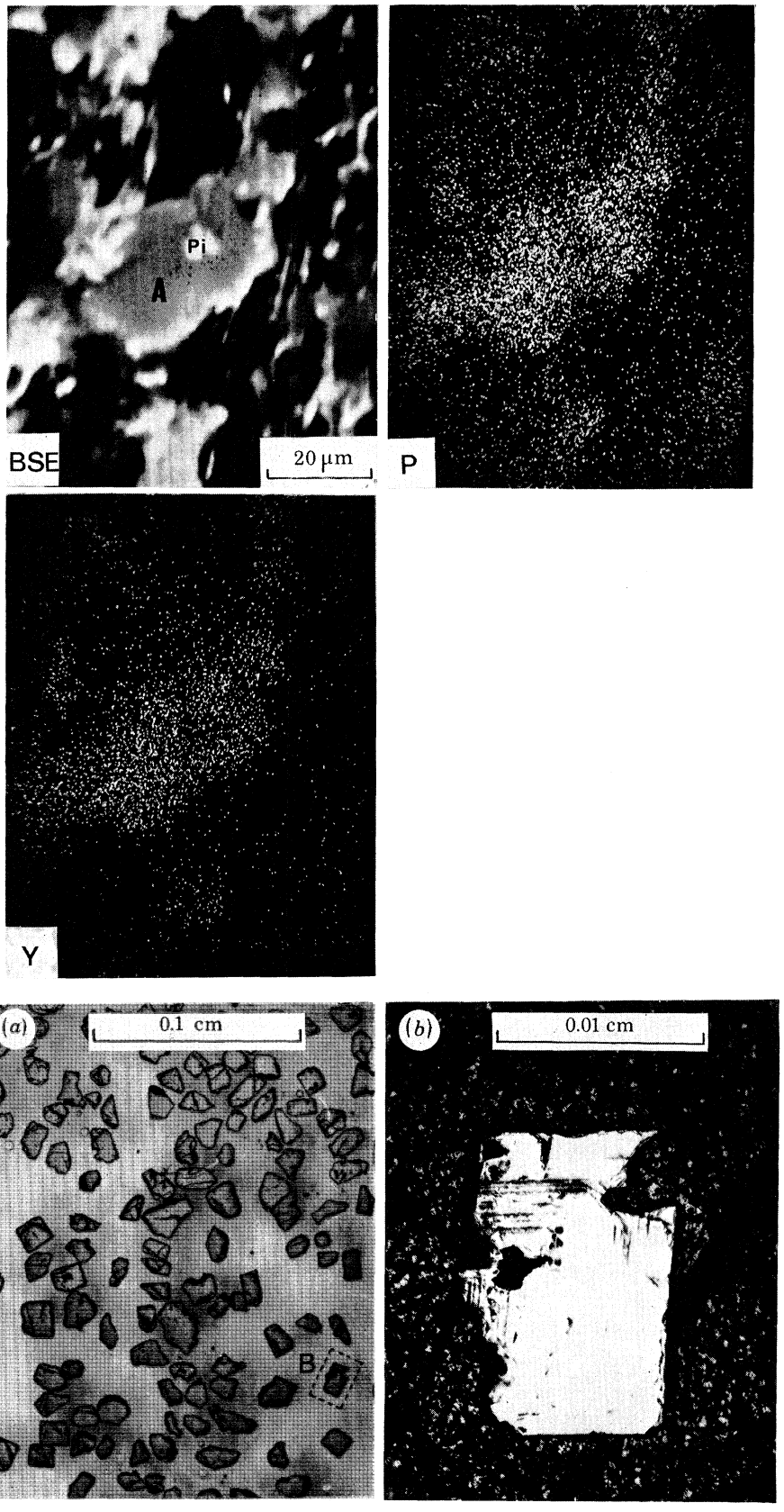

FIGURES 18 AND 19. For description see opposite.

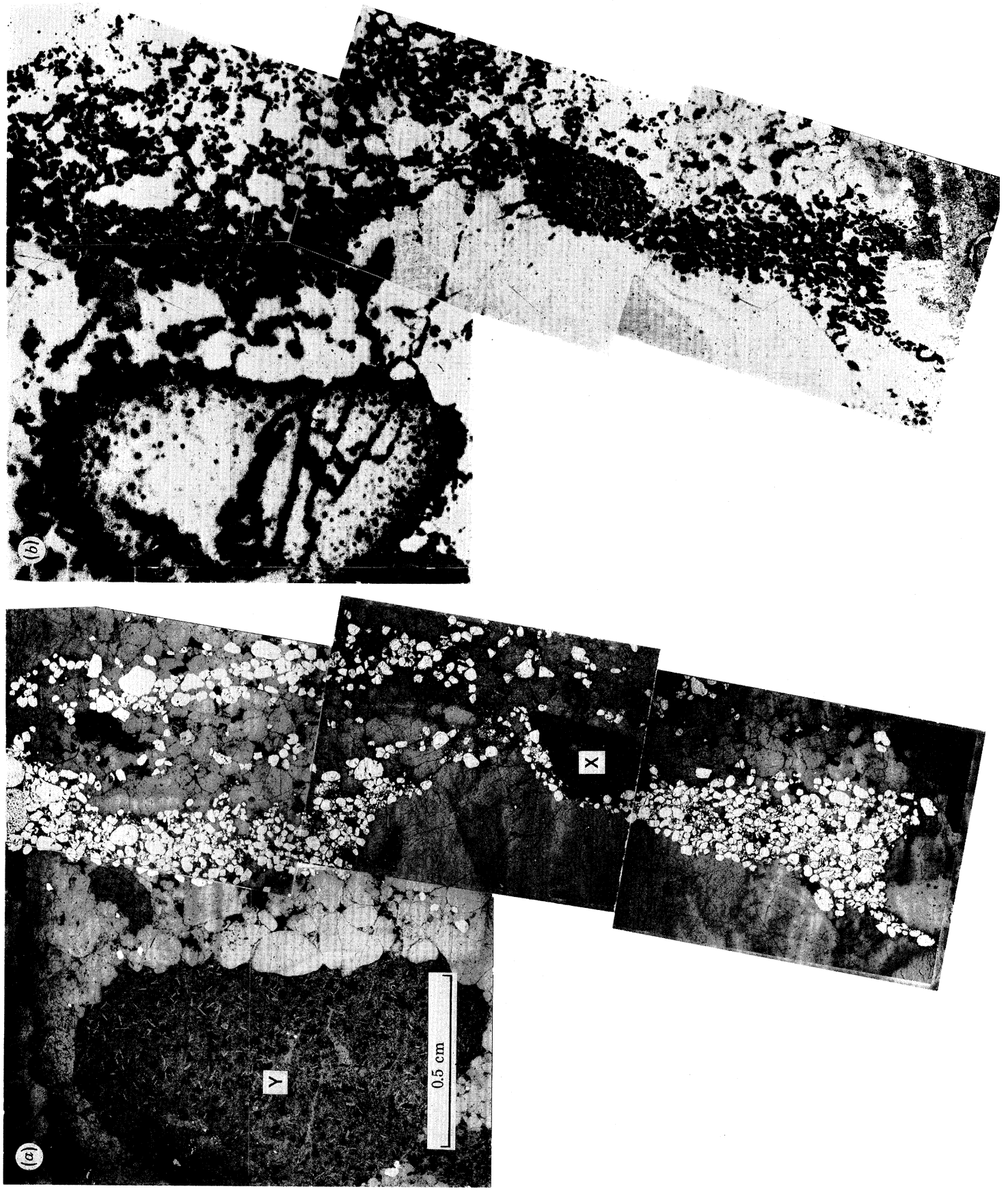
(b)
(a)
X
Y
0.5 cm

cribed by these authors, spherulites of churchite are formed as a coating on siliceous limonite or black manganese oxide. They suggest that the heavy rare earths were concentrated biochemically in the leaves of certain deciduous trees. Stability of the forest floor permitted concentration in the humus layers, from which the churchite coating on existing iron and manganese oxides was derived diagenetically. It seems possible, therefore, that in the Witwatersrand some combination of biochemical and diagenetic processes may have led to the formation of churchite around the fine pitchblende grains in the columnar carbon.

TABLE 1. COMPARISON OF HEAVY RARE EARTH DISTRIBUTION IN XENOTIME, CHURCHITE AND YTTRIUM PHOSPHATE PHASE IN WITWATERSRAND COLUMNAR CARBON RELATIVE TO GADOLINIUM

	Gd	Tb	Dy	Ho	Er	Tm	Yb	Lu
yttrium phosphate phase in carbon†	1	0.49	1.42	—	1.19	—	0.88	—
xenotime‡	1	0.53	5.57	0.72	5.41	1.26	13.03	1.07
churchite§	1	—	1	0.72	1	trace	trace	—
churchite‖	1	—	0.93	0.16	0.53	—	0.60	0.10

† Ratio of $L\alpha$ X-ray peaks from present study.
‡ From an analysis by Jefford (1962, Table 2, No. 1) who quotes similar analyses for other specimens.
§ Ratio of $L\alpha$ X-ray peaks on Bavarian churchite by Henrich (1935).
‖ From the average of two analyses by Pokrovskiy, Tormosova & Kolenko (1965, Table 2).

Origin of the carbonaceous material

Several authors have reported carbonaceous material devoid of mineralization, so neither uranium nor gold performs an essential rôle in its formation. The columnar structures are developed normal to the bedding and it is unlikely therefore that they are metamorphic structures as suggested by Liebenberg (1955). Hallbauer & van Warmelo (1974) later proposed that the structures are a primary feature of the carbonaceous matter. They advanced a theory, further elaborated in Hallbauer, Jahns & Beltmann (1975) and Hallbauer (1975), that the columnar carbonaceous material is the fossilized residue of a Precambrian symbiotic association (designated *Thycomyces lichenoides*) consisting of an algal partner and a fungal organism and occupying areas between a few square centimetres and a few square metres. Treatment of the carbon revealed a skeletal framework of uranium and thorium oxides and of gold, and slow oxidation of the carbon at 500 °C left a heavy-metal fabric, which appears to correspond to the structures described in the present study. Since these metals are most probably deposited in pore spaces in the carbonaceous matter, it is unlikely that they represent the actual skeleton of the 'plant' or are a replacement of any fibrous structure as Hallbauer (1975) suggests. However, the observation that several fine-grained phases containing heavy metals, notably Pb, U, Th, Au and r.e.e., combined with As or S, are closely associated with possible plant-like organisms may have genetic significance for the origin of mineralization in the Witwatersrand, which is discussed later.

DESCRIPTION OF PLATE 10

FIGURE 21. (*a*) Reflected-light and (*b*) corresponding Lexan print, showing a uraniferous pyrite band consisting principally of allogenic pyrite with composite lenticular grains of quartz, kaolinite and pyrophyllite (*x*) and quartz, pyrophyllite and kyanite (*y*). Uranium enrichment is recorded in grain *x*, in the rim and vermicular veinlets in grain *y*, and as a fine dispersion associated with chlorite interstitially to allogenic pyrite grains (see Lexan print). Rare grains of allogenic uraninite are also present. Basal Reef, President Brand, Orange Free State (PTS 842).

Indus river uraninite

Samples of uraninite from the Indus river were analysed by electron probe for comparison with the allogenic uraninite of the Dominion Reef and Witwatersrand Systems, and with a view to assessing the stability of uraninite as a detrital mineral in recent alluvial deposits. The samples had been collected from the Hunza river, a tributary of the Indus in Kashmir (Darnley 1962), and from the Indus alluvium near Hazro, Pakistan (Miller 1963).

The Hunza sample consists of a 99 % pure concentrate in which nearly all the uraninite grains have at least one well-defined crystal face and some show cubic form with little evidence of corrosion. They are in the very fine to fine range of sand size (0.05–0.20 mm) (figure 19, plate 9). Pyrite is present in the concentrate as euhedral cubes, fresh and untarnished, and as concretions. An extensive assemblage of radioactive resistate minerals and sulphides has also been reported (Darnley 1962).

The Hazro samples, which Miller (1963) had reported to contain both uraninite and gold, were also re-examined, involving the preparation of concentrates by vanner, superpanner and heavy liquids. The final concentrate contained in addition to uraninite: pyrite, arsenopyrite, uranothorite and a grain of gold. The sulphides were fresh, but many of the uraninite crystals, with at least one crystal face, had a distinct outer weathered zone, though beneath this they were fresh and homogeneous.

The ThO_2 content of one sample from the Hunza and two from Hazro are shown in figure 10*c*. The three populations exhibit no significant difference, indicating constancy in uraninite composition between sites 300 km apart. The mean UO_2/ThO_2 ratio for the Indus samples is shown in figure 11, to which has been added the ratio for the Dominion Reef uraninite adjusted for uranium and thorium decay to eliminate the effect of the greater age. There is no significant difference between the two uraninite populations after adjustment.

Viljoen (1963) regarded the lack of oxidation of detrital pyrite in the Witwatersrand System as evidence of an atmosphere free of oxygen and Liebenberg (1955) and Grandstaff (1975) considered a non-oxidizing atmosphere was necessary for uraninite transportation. Neither of these conclusions is supported by the evidence from the present-day Indus river, in which as we have seen uraninite, gold, pyrite and other sulphides form a stable assemblage over several hundred kilometres.

Geochemical evidence

Lead content of uraninite and pitchblende

Cumulative frequency curves for the lead content of selected uraninite and pitchblende phases are shown in figure 20. The data fall on four main distributions as follows: (1) relatively young (*ca.* 90 Ma) low-lead allogenic uraninite from the Indus, (2) pitchblende in granular carbon from the Carbon Leader in the Witwatersrand with intermediate lead content, (3) allogenic uraninite in the Witwatersrand and Dominion Reef with high lead content, and (4) pitchblende with high lead content intimately associated with allogenic uraninite in the Witwatersrand.

The intermediate lead content of the pitchblende sample US5 is consistent with the textural observation that this phase is younger than the allogenic uraninite and is formed *in situ* from the diagenesis and metamorphism of the carbonaceous host. The low thorium content of this phase is indicative of a low-temperature solution (thorium being relatively insoluble), from

which uranium was precipitated by absorption on decaying organic matter represented by the carbonaceous material in the section. The highest lead contents are given by the allogenic thorian uraninite phases which are probably a reflection of their greater age. Partial rejuvenation of the allogenic uraninite from the Witwatersrand resulted in the formation of a lead-rich pitchblende in sample 2034. However, the evidence from sample US5 indicates that the presence of allogenic uraninite is not essential for the formation of younger pitchblende, since

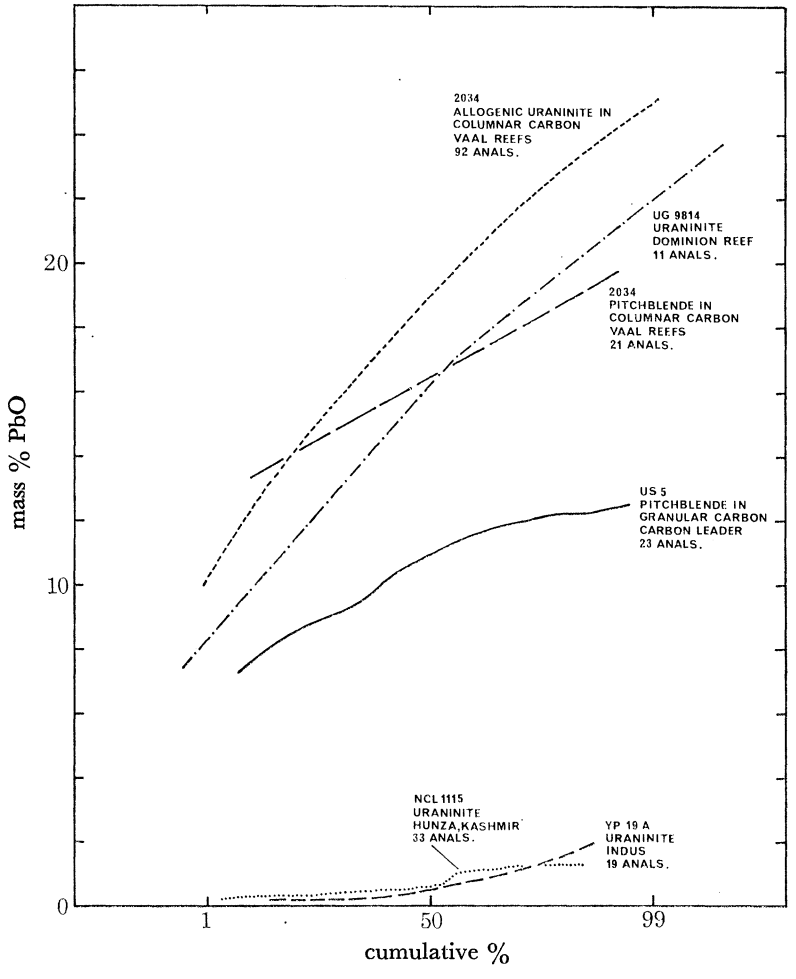

FIGURE 20. Cumulative frequency diagram of the PbO content of uraninite and pitchblende from Dominion Reef, Witwatersrand and Indus river sediments.

it may also form directly from the metamorphism of uranium-enriched carbonaceous material. Younger ages exhibited by pitchblende in the absence of allogenic uraninite should not be generally interpreted therefore as rejuvenation of an older allogenic uraninite, since in the example studied here pitchblende represents direct formation of this phase from a metal-enriched organic substrate; allogenic uraninite was not detected.

Uranium micromapping with thermal neutrons

The distribution of uranium in Witwatersrand and Dominion Reef samples was studied by the fission-track method using Lexan polycarbonate for the registration of fission fragments

from the induced fission of ^{235}U by thermal neutrons, as described by Price & Walker (1963), Kleeman & Lovering (1967) and Bowie, Simpson & Rice (1973). The method is ideal for providing information on the location of uranium in banket-type occurrences. The radioactive bands of interest can usually be included within the breadth of a single polished thin section and radiation doses can be adjusted so as to span concentration ranges. The samples studied here have been subjected to a dose of approximately $5 \times 10^{16} n/cm^2$ in order to obtain a lower detection limit of 0.01 parts/10^6 and track saturation at about 40 parts/10^6. This enables associations of uranium with mineralogical phases to be readily determined when the uranium is below the limits of detection by microprobe.

The results show that uranium is closely confined to discrete horizons both in the banket type and carbonaceous reefs, and that it not only occurs as grains of uraninite but also in a finely disseminated form. Thus uranium is present in pyrite concretions, within lenticular fragments comprising clay-size quartz, kaolinite and pyrophyllite, as a fine disseminated coating on allogenic pyrite grains otherwise uranium free, and, rarely, within dislocations and shears (figures 6, 7, and 21, plate 10).

Both microprobe and fission-track studies show the presence of uranium in the interstitial 7 Å clay phase in the pyrite concretions (figure 8), but fail to detect it in the pyrite itself. A combination of these techniques show that the uranium content of individual concretions is variable within a single reef over a distance of a few millimetres. Whereas some are virtually uranium-free, others are enriched in amounts readily detected by electron microprobe ($>$ 500 parts/10^6). Uranium enrichment occurs only in the rims of some concretions whereas in others, particularly the finer-grained melnikovitic types, the enrichment usually occurs throughout the concretion. This association of uranium with pyrite is particularly striking where it occurs surrounded by an essentially barren quartzitic groundmass, and in cases such as this the evidence for a primary association of uranium with the concretion is strong and probably related to deposition of uranium during the formation of the concretion. The uranium in the rims of concretions was probably absorbed during transport or diagenetically prior to lithification.

Allogenic pyrite is also closely associated with uranium but the uranium in the pyrite is below detection limit and in this case the uranium occurs in a secondary clay mineral forming a marginal overgrowth to the pyrite. This association is particularly well developed in allogenic pyrite occurring in close proximity to a carbonaceous band rich in uranium and gold (PTS 1944, West Driefontein). In this case the uranium was probably deposited *in situ* and subsequently incorporated into the clay mineral overgrowth which formed during diagenesis and metamorphism. This relationship between allogenic pyrite and overgrowths of fine-grained clay minerals and uranium has been recorded widely and is an important control in the deposition of uranium in the Witwatersrand System. The control is specific since uraniferous silicates overgrowing allogenic pyrite occur dispersed through a barren quartzite matrix and are readily identifiable and distinguishable from the textures produced by shearing and later introduction of uranium.

The association of uranium with lenticular to rounded granules consisting of quartz, kaolinite and pyrophyllite has been recognized in many of the Witwatersrand banket-type ores studied here. The uranium occurs disseminated throughout the granules and produces point sources of fission tracks which have not yet been correlated with any specific uranium mineral (figure 21). In some specimens this is the only uranium-bearing mode. The occurrence of these enriched

granules in a barren groundmass indicates that uranium enrichment most probably occurred either before deposition or at the latest during diagenesis. Larger rounded pebbles also occur, some consisting of quartz, pyrophyllite, kyanite and possible illite with secondary spherulitic structures.

In this case uranium occurs on what appears to be a leached and weathered margin and along a vermicular veinlet structure within the pebble. Enrichment in uranium during transport and diagenesis related to weathering of the pebble rim (figure 21) seems to be the most likely explanation of this occurrence. Regional metamorphism has tended to reduce the thickness of the uraniferous rim, which is best developed where weathered pebbles are relatively unaltered.

Neutron activation analysis of whole rock samples

Instrumental neutron activation analysis of whole-rock samples was undertaken as an adjunct to the mineralogical studies utilizing a method developed by Plant, Goode & Herrington (1976).

The results are given in table 2 and demonstrate the increase in U/Th ratios from the Dominion to the Vaal reefs in the Witwatersrand basin. Freddies Reef, East Geduld, and Daggafontein are somewhat higher and similar to one another, whereas samples from West Driefontein, dominated by carbonaceous matter, have the highest ratios. Twenty-four additional elements obtained by this method on the same sample are presented for comparison with uranium and thorium. This gradational variation in the U/Th ratio is an approximate measure of the depositional environment. The high-energy environment has a low ratio and the low-energy environment a high ratio with continuous variation between the two.

Bimodal nature of the uranium mineralization

The occurrence of allogenic grains of uraninite in the Dominion Reef (Taylor, Bowie & Horne 1962) and the Witwatersrand (Liebenberg 1955; Grandstaff 1975) is well established. This phase occurs in the Dominion Reef in association with resistate phases such as garnet, monazite, cassiterite, zircon, allogenic sulphides, rare authigenic sulphides and gold. The similarity of this assemblage with modern gravels on banks in the Indus is notable, although uraninite in the Indus is at present sub-economic (Miller 1963). In the Witwatersrand System the characteristically lower content of allogenic uraninite and rounded resistate phase, the relatively greater importance of concretionary pyrite and the appearance of carbonaceous matter as an important accessory or even dominant phase, represent a markedly different style of mineralization.

The general similarity of the median values of the UO_2/ThO_2 ratios between 14 and 20 for allogenic uraninite from the Indus Valley, Dominion Reef and Witwatersrand is most significant. However, the pitchblende associated with granular carbonaceous material in the Witwatersrand has a much higher median ratio of about 32 and this is a distinct and separate phase of mineralization differing from the allogenic uraninite texturally, compositionally, and in its close association with carbonaceous matter and gold.

The fission track studies have clearly indicated an association of uranium in Witwatersrand sediment with clay minerals occurring individually or intergrown with, or overgrowing, pyrite, and in many cases this association has the appearance of a primary, essentially syngenetic, relationship unaffected by appreciable uranium remobilization.

Evidence of this type from Witwatersrand sediments provides support for the existence of some uranium in solution in the Basin during sedimentation and diagenesis as discussed by Pretorius (1975). The uranium would be highly mobile as the soluble uranyl ion, UO_2^{2+}, which would subsequently be absorbed, reduced, and precipitated by organic-rich muds probably aided by and associated with the simultaneous reduction of sulphate by bacteria as proposed by Trudinger (1971):

$$SO_4^{2-} + 8e + 10H^+ \rightarrow H_2S + 4H_2O.$$

The hydrogen sulphide formed would subsequently react with other metals in solution such as iron and lead to form the authigenic intergrowths of pyrite and galena with clay minerals, gold and uranium observed in the sediments.

TABLE 2. NEUTRON ACTIVATION ANALYSIS (IN PARTS/10^6 EXCEPT WHERE STATED)

sample location	rock sample	Na	K	Sc	Cr	Fe%	Co	Zn	As	Rb	Ag	Cd	Sb	Cs
Dominion Reefs	5A 2006/2133	2.19%	< 2000	38	< 400	10.2	570	< 300	3800	< 100	< 40	< 100	28	< 5
	BR8N2(B) 2004/2134	< 200	6600	24	249	7.31	260	< 300	340	< 200	< 35	< 100	< 6	< 5
	BR6N4(A) 2018/2135	< 200	< 2000	30	374	4.96	425	< 300	3100	< 200	< 40	< 100	< 10	< 6
	BR7N1(B) 1998/2136	< 1000	< 2000	32	297	7.63	420	< 300	3600	< 200	< 40	< 100	19	< 10
Vaal Reefs	UR21A 2055/2121	< 800	< 2000	10	1400	6.56	260	344	605	< 100	< 20	< 100	25	< 5
	UR3 2034/2122	< 1000	< 2000	13	450	2.80	216	< 350	1200	< 200	< 40	< 100	53	< 6
	UR5 2039/2123	980	< 2000	7	890	4.89	229	< 160	670	< 200	< 40	< 100	27	7
	UR16 2049/2124	990	< 2000	8	315	1.65	120	< 160	370	< 100	< 30	< 100	21	5
Freddies Reef	FW4 2105/2137	52	< 2000	4.2	850	1.77	108	440	430	< 100	< 15	< 100	6	< 5
	FW2 2103/2138	66	< 2000	46	760	3.17	123	354	620	< 80	22	< 100	10	< 5
East Geduld	EG4 2064/2139	330	5900	6.7	2300	5.09	200	366	640	< 100	< 15	< 100	15	< 5
	EG18 2078/2140	190	930	4.6	560	3.63	117	295	140	< 100	< 40	< 100	< 5	< 5
Daggafontein	26 1995/2128	94	< 2000	6	152	6.76	312	239	336	< 100	24	< 100	< 5	< 3
	27 1996/2129	256	< 2000	18	1200	7.67	219	< 800	296	< 100	< 40	< 100	< 5	< 3
	KE4/7 1975/2130	220	< 2000	3	115	0.21	21	220	29	< 50	< 15	< 100	< 5	< 3
	K6F12/11 1979/2131	86	< 2000	8	244	1.19	43	818	134	< 100	< 15	< 100	< 5	< 3
	KG6/10 1978/2132	520	2200	11	650	2.79	55	< 100	120	< 70	< 15	< 100	6	< 3
West Driefontein	8A 1959/2125	387	< 2000	7.5	1040	4.93	140	360	450	< 100	46	< 100	9	< 3
	4B 1950/2126	204	< 2000	4	235	4.34	59	264	46	< 50	39	< 100	< 5	< 3
	5 1951/2127	< 400	< 2000	4	84	2.38	14	463	60	< 150	130	< 100	7	< 3

TABLE 2 (*cont.*)

sample location	rock sample	Ba	La	Ce	Nd	Sm	Eu	Tb	Lu	Hf	Ta	Au	Th	U	U/Th
Dominion Reefs	5A														
	2006/2133	< 500	1.3%	1200	1000	445	< 2	20	14	< 10	410	3	809	3900	4.8
	BR8N2(B)														
	2004/2134	< 1000	906	1200	850	285	12	16	10	15	240	9	620	2300	3.7
	BR6N4(A)														
	2018/2135	< 1000	1400	2200	910	335	12	17	11	19	450	2	753	2300	3.1
	BR7N1(B)														
	1998/2136	< 1000	1100	1800	1270	600	20	15	18	18	450	5	970	5400	5.6
Vaal Reefs	UR21A														
	2055/2121	< 1000	260	700	1500	450	20	8	13	22	8	154	477	4500	9.4
	UR3														
	2034/2122	< 1000	475	900	2800	850	37	24	22	30	< 100	218	821	8400	10.2
	UR5														
	2039/2123	< 1000	248	350	860	200	17	6	6	36	7	69	298	2100	7.1
	UR16														
	2049/2124	< 1000	172	500	940	250	15	6	8	11	< 5	214	273	2700	9.9
Freddies Reef	FW4														
	2105/2137	< 500	59	260	170	60	4.7	< 5	< 3	18	30	90	52	685	13.2
	FW2														
	2103/2138	< 500	68	135	195	65	5.3	< 5	< 3	< 20	30	115	80	765	9.6
East Geduld	EG4														
	2064/2139	< 500	41	< 200	280	< 10	3.6	5	< 3	17	6	118	40	510	12.8
	EG18														
	2078/2140	< 500	57	80	73	12	1.2	2	< 3	11	4	1.5	20	75	3.8
Daggafontein	26														
	1995/2128	< 1000	44	< 100	227	75	1.5	< 2	< 1	4	15	173	71	895	12.6
	27														
	1996/2129	< 1000	42	< 10	400	160	8	3	< 3	8	20	132	102	2000	19.6
	KE4/7														
	1975/2130	< 1000	20	22	9	6	1	< 2	< 1	< 2	< 5	0.4	< 5	43	—
	K6F12/11														
	1979/2131	< 1000	16	45	112	30	1.5	< 2	< 1	2	2	28	< 10	337	—
	KG6/10														
	1978/2132	< 300	22	55	43	20	2	< 2	< 1	2	30	11	15	180	12.0
West Driefontein	8A														
	1959/2125	< 1000	47	< 300	88	40	3	< 2	< 5	19	50	428	40	460	11.5
	4B														
	1950/2126	< 1000	25	< 10	340	100	6	3	< 3	7	< 5	221	75	1400	18.7
	5														
	1951/2127	< 1000	69	< 30	454	140	7	16	4	< 5	< 5	444	99	1500	15.2

The most likely modes of introduction of uranium, gold and sulphate in solution are the complex fault system of the Witwatersrand basin and dissolution of coexisting detrital minerals. Some of the sulphate would have been precipitated in close proximity to hot springs at the margin of the Basin, but some gold and uranium would have remained in solution, perhaps with the aid of metal-organic complexes (Vine, Swanson & Bell 1958; Ling Ong & Swanson 1974; Boyle, Alexander & Aslin 1975). The gold and uranium in solution would have been carried out into the Basin to be precipitated together on the distal portions of the alluvial fans by the action of decaying organic matter.

This process accounts for the observed primary distribution of uranium and gold other than the purely detrital material, and explains the separation of uranium and thorium in the

progression from the higher energy Dominion Reef to the lower energy Witwatersrand environment. Though relatively unimportant in the higher energy banket type of mineralization, deposition from solution through the agency of organic matter would seem to be responsible for major economic concentrations of both uranium and gold over large areas in the Witwatersrand Basin in the lower energy Carbon Leader type of mineralization.

Conclusions

The overall control of the uranium mineralization in the Witwatersrand and Dominion Reef Systems is the presence of a depositional basin overlying an Archaean craton in which very early differentiation on the model proposed by Fyfe (1970, 1973) and amplified by Moorbath (1975) enriched the upper crust in oxyphile metals including uranium. This process has been considered by Bowie (1970) as a fundamental control in the delineation of metallogenic provinces and hence in the distribution on a global scale of economic concentrations of uranium.

In this Basin, uranium was deposited in two ways, as detrital allogenic uraninite and by precipitation from solution. The detrital components were concentrated in the higher energy conglomerate environment of the Dominion Reef and proximal parts of the Witwatersrand basin. The solution components including uranium and gold were precipitated under reducing conditions through the agency of decaying organic matter in the lower energy or distal regions of the Basin, giving rise through diagenesis and metamorphism to such uraniferous horizons as the Carbon Leader of the West Wits, which are not directly related to known palaeogeographical channels. It can now be clearly demonstrated that relatively small amounts of thorium increases the resistance to attrition and oxidation to the extent that a thorian uraninite with 1 % or more thorium oxide can survive as river detritus under present-day atmospheric conditions. All of the uraninite grains from the Witwatersrand Basin considered to be of detrital origin contain 1 % thorium oxide or more, hence it is unnecessary to postulate a reducing atmosphere, indeed the retention of sulphate and uranyl ions in solution would seem to require the existence of an oxidizing atmosphere in the model proposed here for the deposition of uranium from solution.

This conclusion therefore suggests that the occurrence of pebble conglomerates with detrital uraninite and pitchblende deposited from solution may have a more widespread occurrence throughout geological time than hitherto suspected, provided the necessary geological criteria for their formation are met.

The writers wish to acknowledge the assistance of I. R. Basham and D. A. Briggs in preparing heavy mineral concentrates from the alluvium samples from Hazro, Indus river. B. R. Skilton and J. A. T. Smellie prepared polished thin sections and M. J. Cope prepared Lexan prints. D. Atkin provided X-ray diffraction identification. In particular we wish to acknowledge helpful discussions with S. H. U. Bowie, A. G. Darnley and J. E. T. Horne. We are indebted to A. G. Darnley and J. M. Miller for the Indus river samples and to S. H. U. Bowie, A. G. Darnley and H. C. M. Whiteside for samples from the Dominion Reef and Witwatersrand sediments. C. Goode and J. Herrington of the Herald Reactor Group, A. W. R. E., Aldermaston, are thanked for the provision of whole-rock instrumental neutron activation analyses and for irradiation of sectioned material for induced fission-track analysis. Jane Plant is thanked

for helpful discussions on solution chemistry, and R. J. Howarth for advice on statistical methods. This work forms part of the research programme of the Institute of Geological Sciences and is published with the approval of the Director.

References (Simpson & Bowles)

Bourret, W. 1973 *First uranium report – Witwatersrand, South Africa.* Utah International, Inc. San Francisco. 51p.

Bowie, S. H. U. 1970 Some geological concepts for consideration in the search for uranium provinces and major uranium deposits. In *Uranium exploration geology* (Proceedings of a Panel, Vienna 1970), IAEA, Vienna, 285–300.

Bowie, S. H. U., Simpson, P. R. & Atkin, D. A. 1975 Reflectance measurements in monochromatic light on the Bowie–Taylor suite of 103 ore minerals. *Fortschr. Miner.* **52**, 567–582.

Bowie, S. H. U., Simpson, P. R. & Rice, C. M. 1973 Application of fission-track and neutron activation methods to geochemical exploration. In *Geochemical Exploration* 1972, pp. 359–372. Inst. Min. Metal. London.

Bowles, J. F. W. 1975 An automatic data-handling system for quantitative X-ray microprobe analysis. *Rep. Inst. Geol. Sci.* No. 75/9. 14 pp.

Bowles, J. F. W. (in preparation). Quantitative energy dispersive analysis of ore minerals.

Boyle, R. W., Alexander, W. M. & Aslin, G. E. M. 1975 Some observations on the solubility of gold. *Geol. Surv. Can. Pap.* **75–24**, 6 pp.

Claringbull, G. F. & Hey, M. H. 1953 A re-examination of churchite. *Mineral. Mag.* **30**, 211–217.

Coetzee, F. 1965 Distribution and grain-size of gold, uraninite, pyrite and certain other heavy minerals in gold-bearing reefs of the Witwatersrand Basin. *Trans. geol. Soc. S. Afr.* **68**, 61–88.

Cooper, R. A. 1923 Mineral constituents of Rand concentrates. *Chem. met. miner. Soc. S. Afr.* **24**, 90–95.

Darnley, A. G. 1962 Detrital uraninite from the Hunza River, Kashmir. Age Determination Rep. No. 22. *Geol. Surv. G.B. Atomic Energy Division* (unpublished).

Davidson, C. F. & Bowie, S. H. U. 1951 On thucholite and related hydrocarbon-uraninite complexes. *Bull. Geol. Surv. G.B.* **3**, 1–18.

Drake, M. J. & Weill, D. F. 1972 New rare earth element standards for electron microprobe analysis. *Chem. Geol.* **10**, 179–181.

Feather, C. E. & Koen, G. M. 1975 The mineralogy of the Witwatersrand reefs. *Miner. Sci. Eng.* **7**, 189–224.

Frondel, C. 1958 Systematic mineralogy of uranium and thorium. *Bull U.S. Geol. Surv.* 1064.

Fyfe, W. S. 1970 Some thoughts on granitic magmas. In *Mechanism of igneous intrusion* (eds G. Newall & N. Rast). *Geol. J.* Special Issue No. **2**, 201–216.

Fyfe, W. S. 1973 The granulite facies, partial melting and the archaean crust. *Phil. Trans. R. Soc. Lond.* A **273**, 457–462.

Grandstaff, D. W. 1975 Microprobe analyses of uranium and thorium in uraninite from the Witwatersrand, South Africa, and Blind River, Ontario, Canada. *Trans. geol. Soc. S. Afr.* **77**, 291–294.

Graton, L. C. 1930 Hydrothermal origin of the Rand gold deposits: part I – testimony of the conglomerates. *Econ. Geol.* **25**, supp. to No. 3, 185 pp.

Hallbauer, D. K. & Van Warmelo, K. T. 1974 Fossilized plants in thucholite from Precambrian rocks of the Witwatersrand, South Africa. *Precambrian Res.* **1**, 199–212.

Hallbauer, D. K., Jahns, H. M. & Beltmann, H. A. 1975 Morphological and anatomical observations on some Precambrian plants from the Witwatersrand, South Africa. *Res. Rep.* **49/75**, *Chamber of Mines of S. Afr.* 22 pp.

Hallbauer, D. K. 1975 The plant origin of the Witwatersrand carbon. *Miner. Sci. Eng.* **7**, 111–131.

Henrich, F. 1935 A mineral occurring in Germany with rare earths as essential constituents. *J. Prakt. Chem.* **142**, 1–5.

Jefford, G. 1962 Xenotime from Rayfield, N. Nigeria. *Am. Miner.* **47**, 1467–1473.

Köppel, V. H. & Saager, R. 1974 Lead isotope evidence on the detrital origin of Witwatersrand pyrites and its bearing on the provenance of the Witwatersrand gold. *Econ. Geol.* **69**, 318–331.

Kleeman, J. D. & Lovering, J. F. 1967 Uranium distribution studies by fission track registration in Lexan plastic prints. *Atomic Energy Aust.* **10**, 3–8.

Liebenberg, W. R. 1955 The occurrence and origin of gold and radioactive minerals in the Witwatersrand System, the Dominion Reef, the Ventersdorp Contact Reef and the Black Reef. *Trans. geol. Soc. S. Afr.* **58**, 101–223.

Ling Ong, H. & Swanson, V. W. 1974 Natural organic acids in the transportation deposition and concentration of gold. *Colorado Sch. Mines Q.* **69**, 395–425.

Mason, P. K., Frost, M. T. & Reed, S. J. B. 1969 B.M.–I.C.–N.P.L. Computer programs for calculating corrections in quantitative X-ray microanalysis. National Physical Laboratory I.M.S. Rep. No. 2 (unpublished).

Miller, J. M. 1963 Uraninite-bearing placer deposits in the Indus alluvium near Hazro, Pakistan. Rep. No. 254 *Geol. Surv. G.B. Atomic Energy Division* (unpublished).

Milton, C., Murata, K. J. & Knechtel, M. M. 1944 Weinschenkite, Yttrium phosphate dihydrate, from Virginia. *Am. Miner.* **29**, 92–107.

Moorbath, S. 1975 The geological significance of Early Precambrian Rocks. *Proc. geol. Ass.* **86**(3), 259–279.

Plant, J., Goode, C. & Herrington, T. 1976 An instrumental neutron activation method for multi-element mapping. *J. geochem. Explor.* **6** (3), 299–319.

Pokrovskiy, P. V., Tormosova, G. F. & Kolenko, L. I. 1965 Weinschenkite from the Central Urals. *Dokl. Earth Sci. Sect.* **162**, 133–136. Transl. from *Dokl. Akad. Nauk SSSR* **162**, 173–175.

Pretorius, D. A. 1975 The depositional environment of the Witwatersrand gold fields. A chronological review of speculations and observations. *Miner. Sci. Eng.* **7**, 18–47.

Price, P. B. & Walker, R. M. 1963 A simple method of measuring low uranium concentrations in natural crystals. *Appl. Phys. Lett.* **2**, 23–5.

Ramdohr, P. 1958 New observations on the ores of the Witwatersrand in South Africa and their genetic significance. *Trans. geol. Soc. S. Afr.* (Annexure) **61**, 1–50.

Robertson, D. S. 1974 Basal Proterozoic units as fossil time markers and their use in uranium prospection. In *Formation of uranium ore deposits*, pp. 495–512. Vienna: IAEA.

Saager, R. & Mihálik, P. 1967 Two varieties of pyrite from the Basal Reef of the Witwatersrand System. *Econ. Geol.* **62**, 719–731.

Saager, R. 1970 Structures in pyrite from the Basal Reef in the Orange Free State Gold-field. *Trans. geol. Soc. S. Afr.* **73**, 31–46.

Taylor, K., Bowie, S. H. U .& Horne, J. E. T. 1962 Radioactive minerals in the Dominion Reef. *Mineral. Mag.* **107**, 329–332.

Tourtelot, H. A. 1968 The hydraulic equivalance of grains of quartz and heavier minerals and implications for study of placers. *U.S. geol. Surv. Prof. Pap.* 594F.

Trudinger, P. A. 1971 Microbes, metals and minerals. *Miner. Sci. Eng.* **4**, 13–25.

Viljoen, R. P. 1963 Petrographic and mineragraphic aspects of the Main Reef and Main Reef Leader on the Main-Bird Series, Witwatersrand System. Unpublished M.Sc. Thesis, University of the Witwatersrand, Johannesburg.

Vine, J. D., Swanson, V. E. & Bell, K. G. 1958 The role of humic acids in the geochemistry of uranium. *Proc. Second U.N. Int. Conf. on Peaceful uses of Atomic Energy* **2**, 187–191.

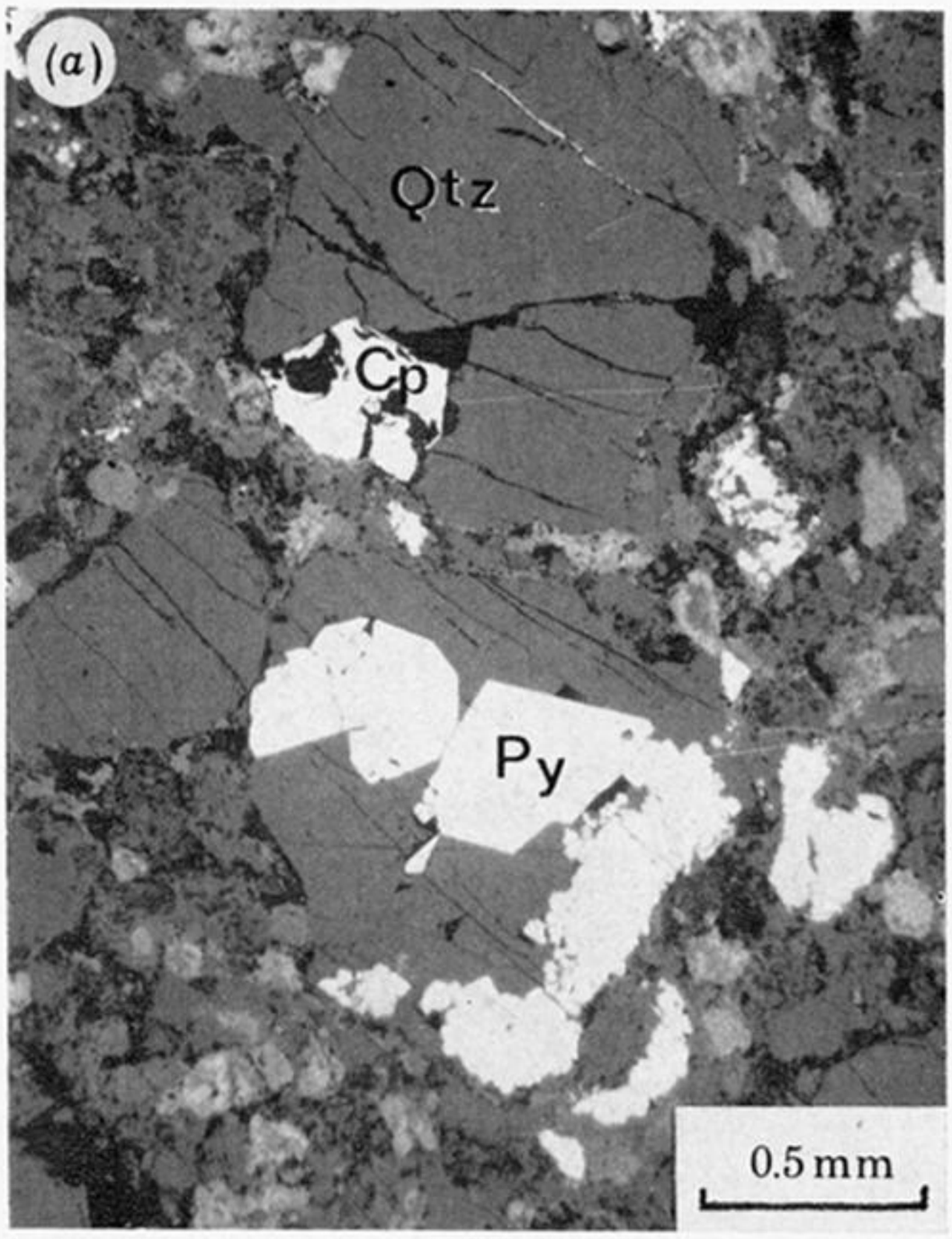

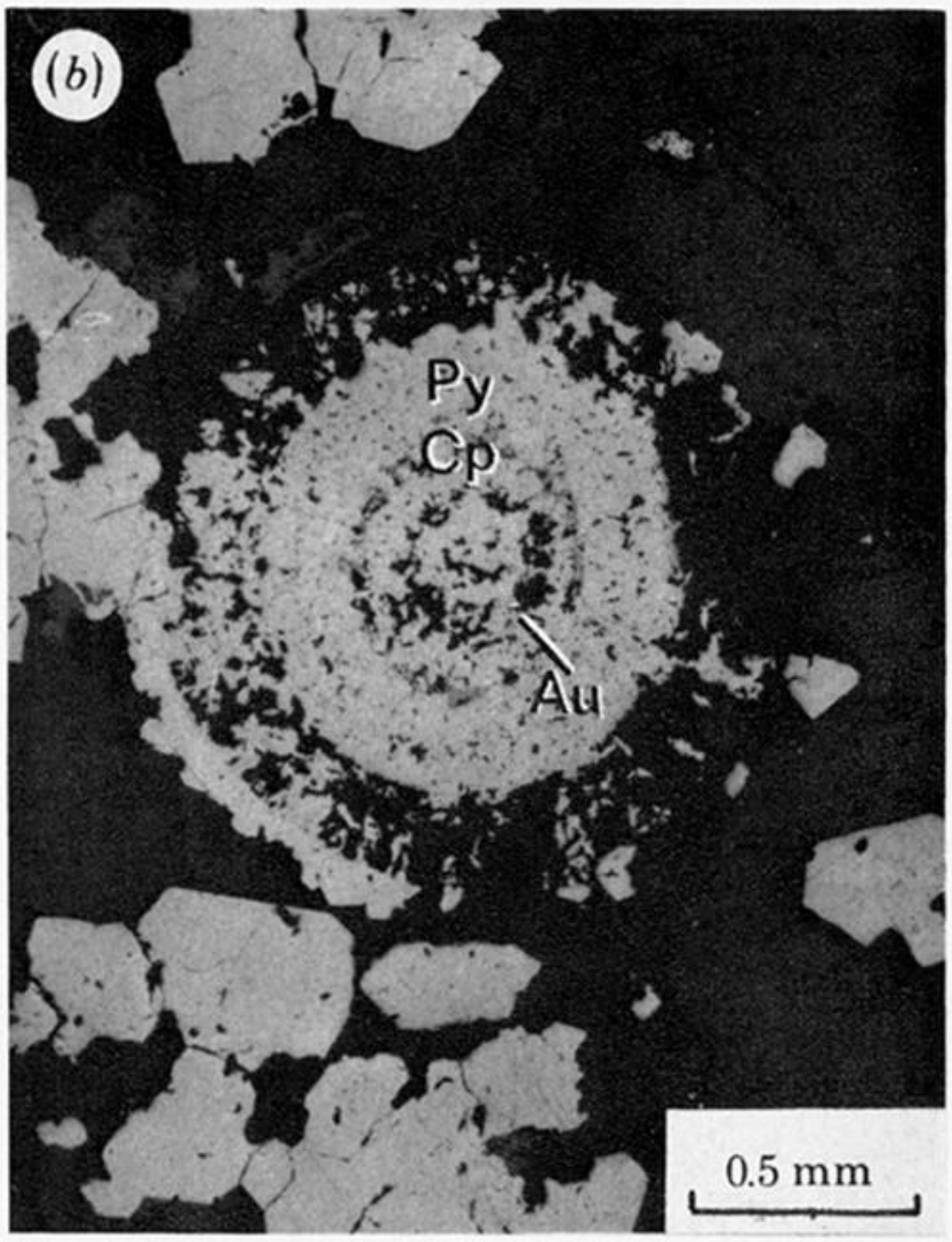

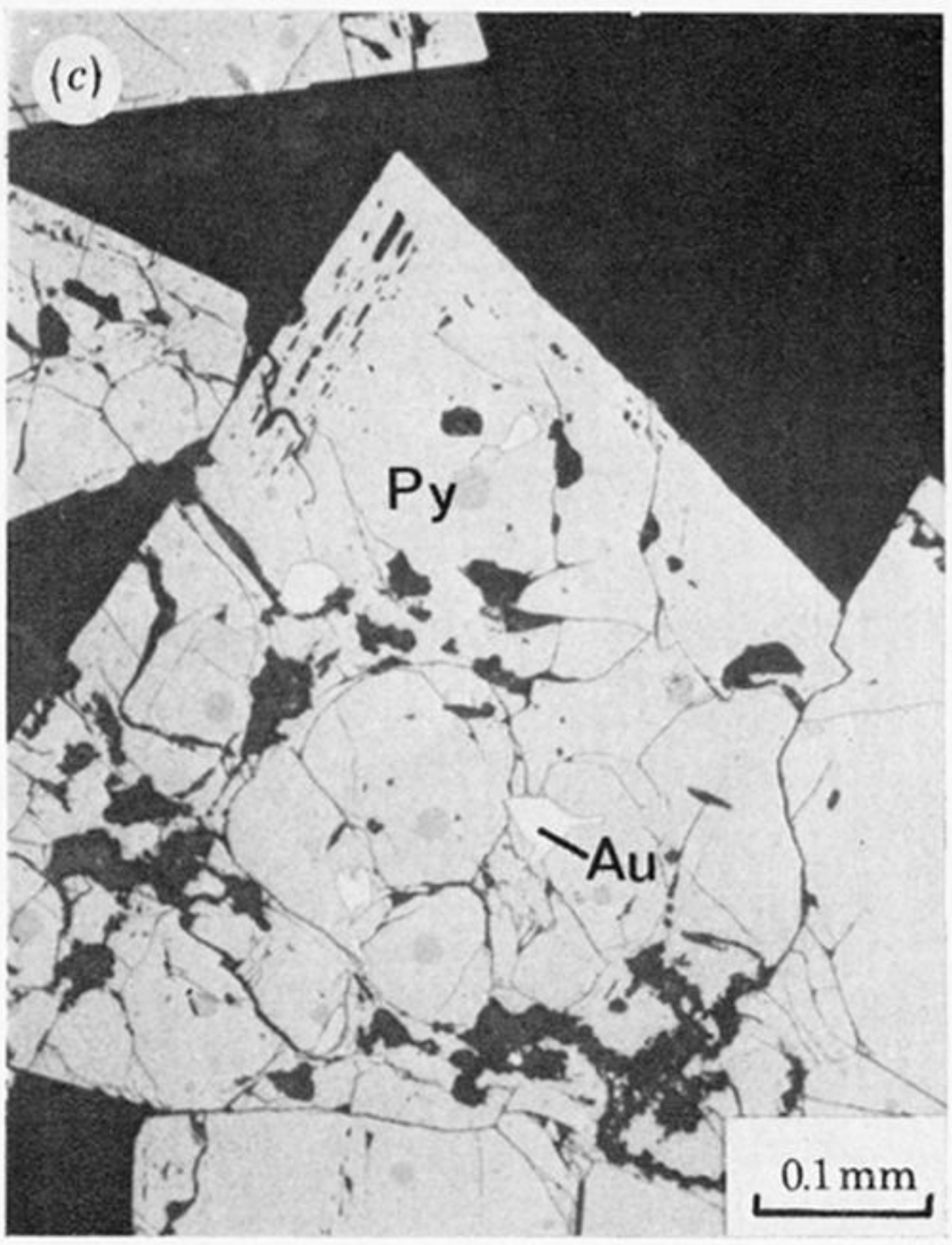

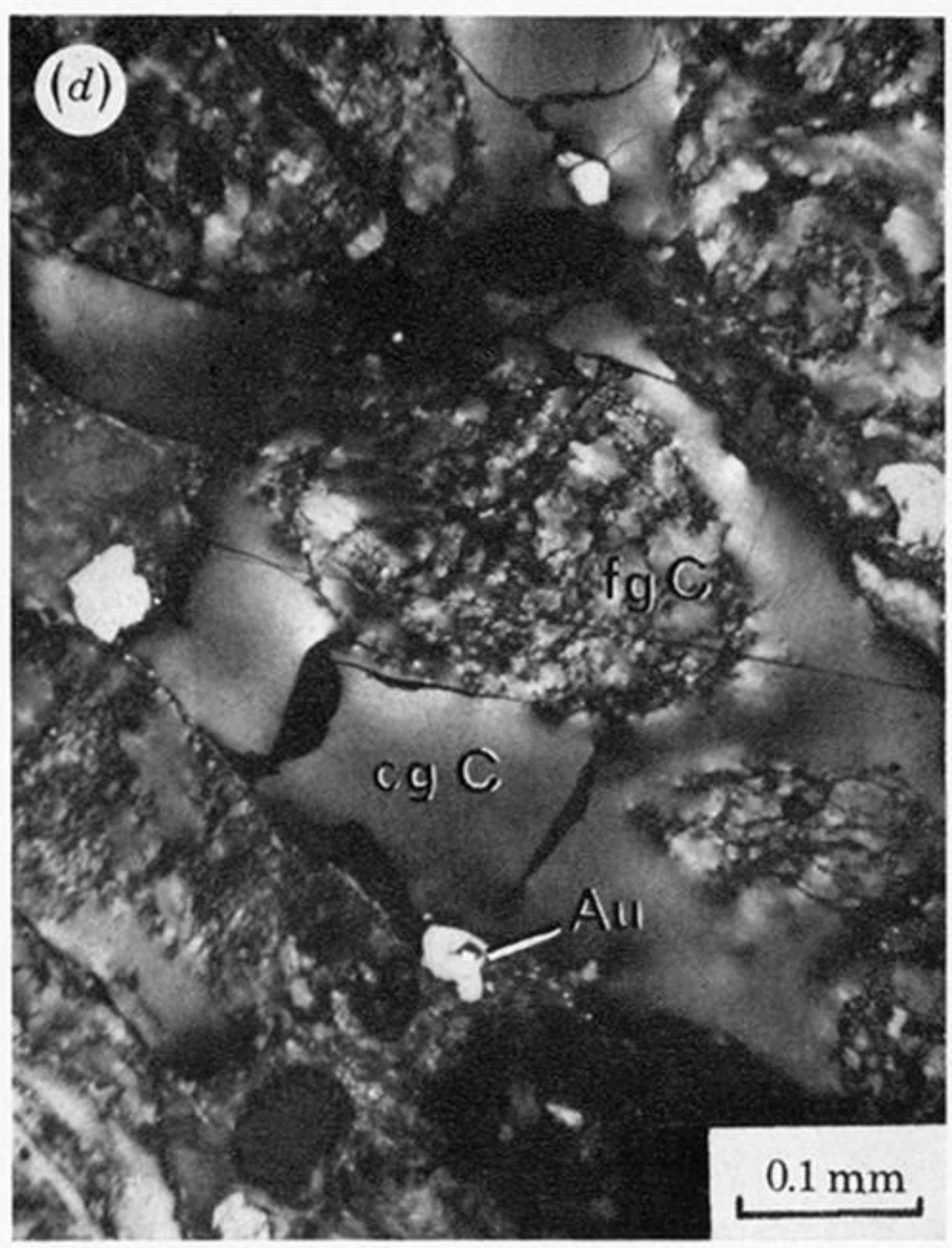

FIGURE 3 (*a*) Banket ore sample showing allogenic pyrite (Py), chalcopyrite (Cp) and quartz (Qtz); Dominion Reef, (US1273C), reflected light, air.

(*b*) Concretionary pyrite of spherical type composed of alternate layers of pyrite (Py) and chalcopyrite (Cp) with a grain of gold (Au). Silicates occur in the body of the concretion and particularly in the rim, as well as in the porous matrix (black). West Driefontein, West Wits (PTS 1966), reflected light, oil.

(*c*) Authigenic reconstituted pyrite (Py) containing gold (Au). West Driefontein, West Wits, (PTS 1958), reflected light, oil.

(*d*) Carbonaceous matter showing coarse (cgC) and fine-grained (fgC) carbon, with gold (Au). Carbon Leader, West Wits (US 5), reflected light, oil.

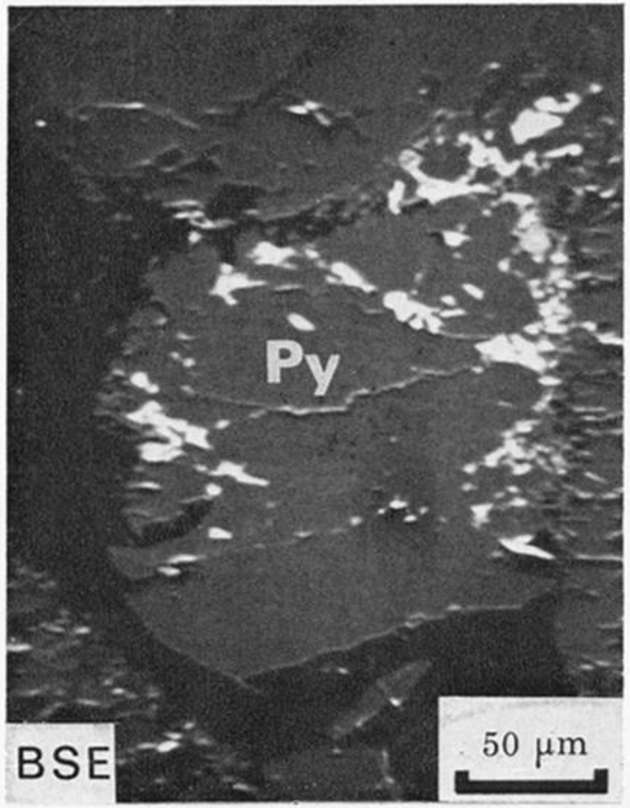

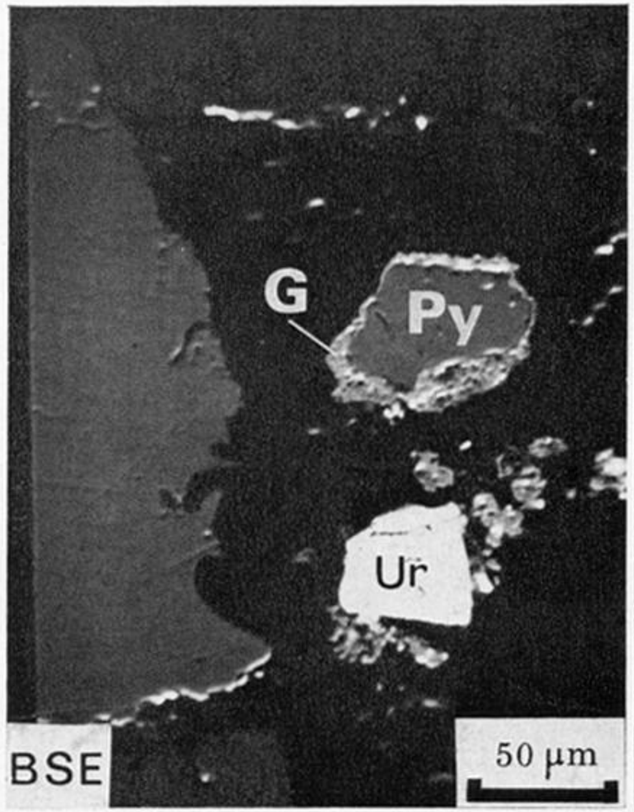

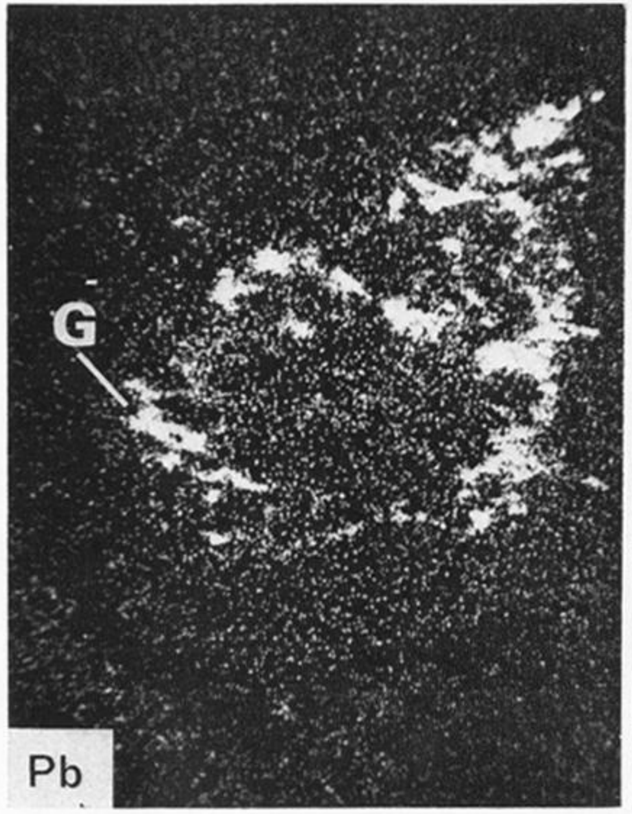

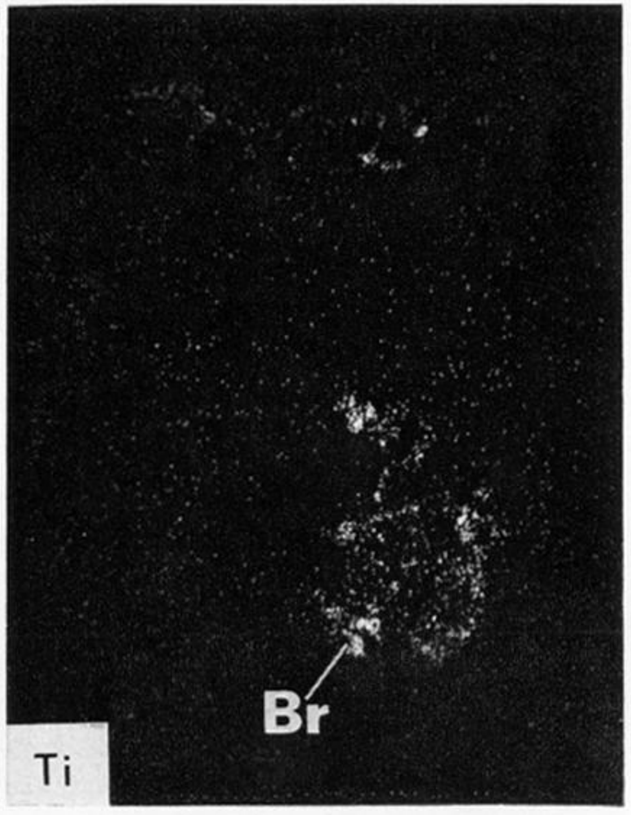

FIGURES 4 AND 5. For description see opposite.

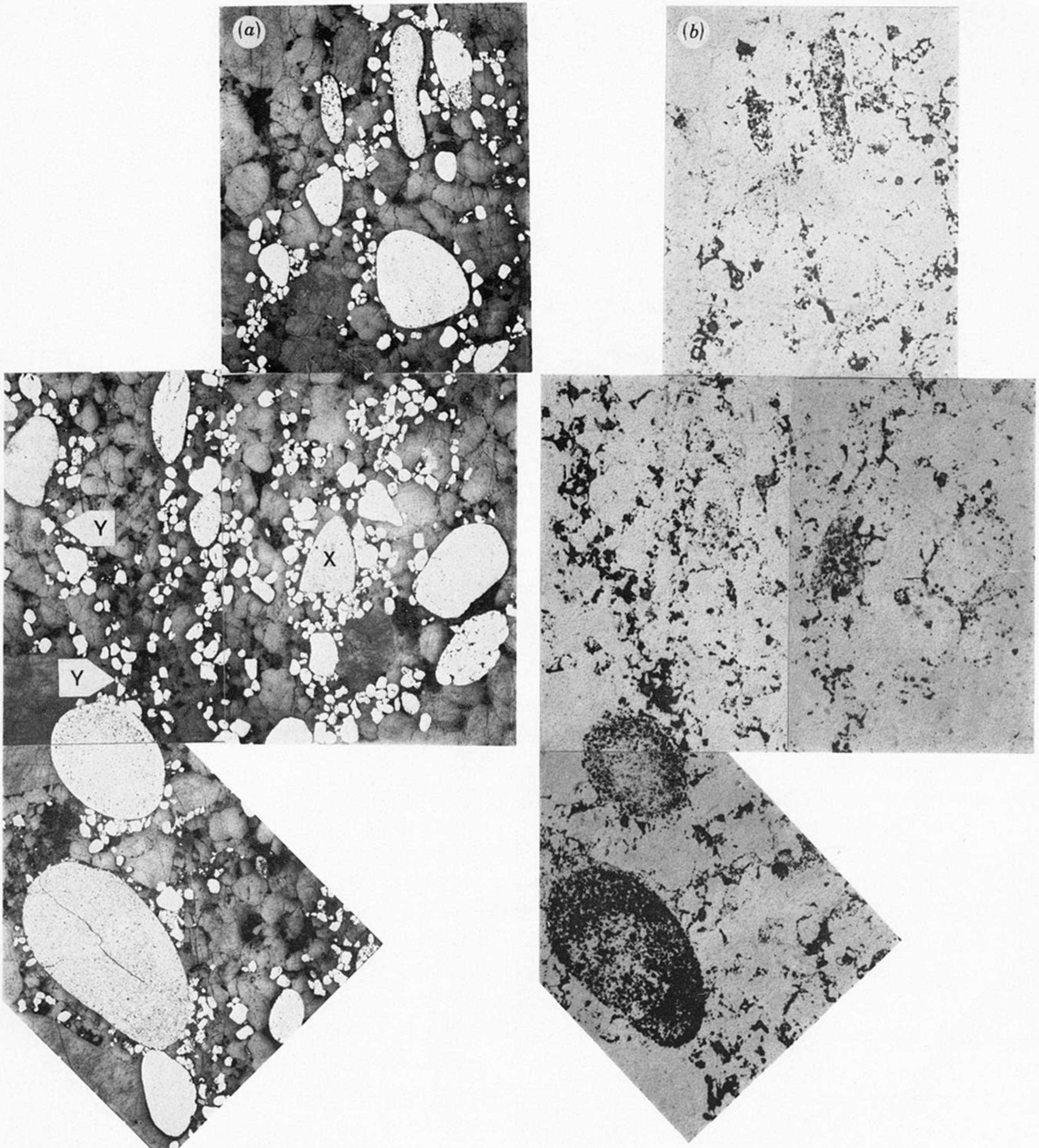

FIGURE 6. (*a*) Reflected light and (*b*) corresponding Lexan print showing a uraniferous pyritic band consisting of larger concretionary and smaller allogenic pyrite (white). Uranium is enriched in some concretionary pyrite grains but not in others (see Lexan print). One concretionary pyrite grain (*X*) has been fractured and further worn before deposition. Uranium present in the matrix is accounted for by allogenic grains of uraninite (*Y*), and interstitial clay minerals; Basal Reef, President Brand, Orange Free State (PTS 2463B).

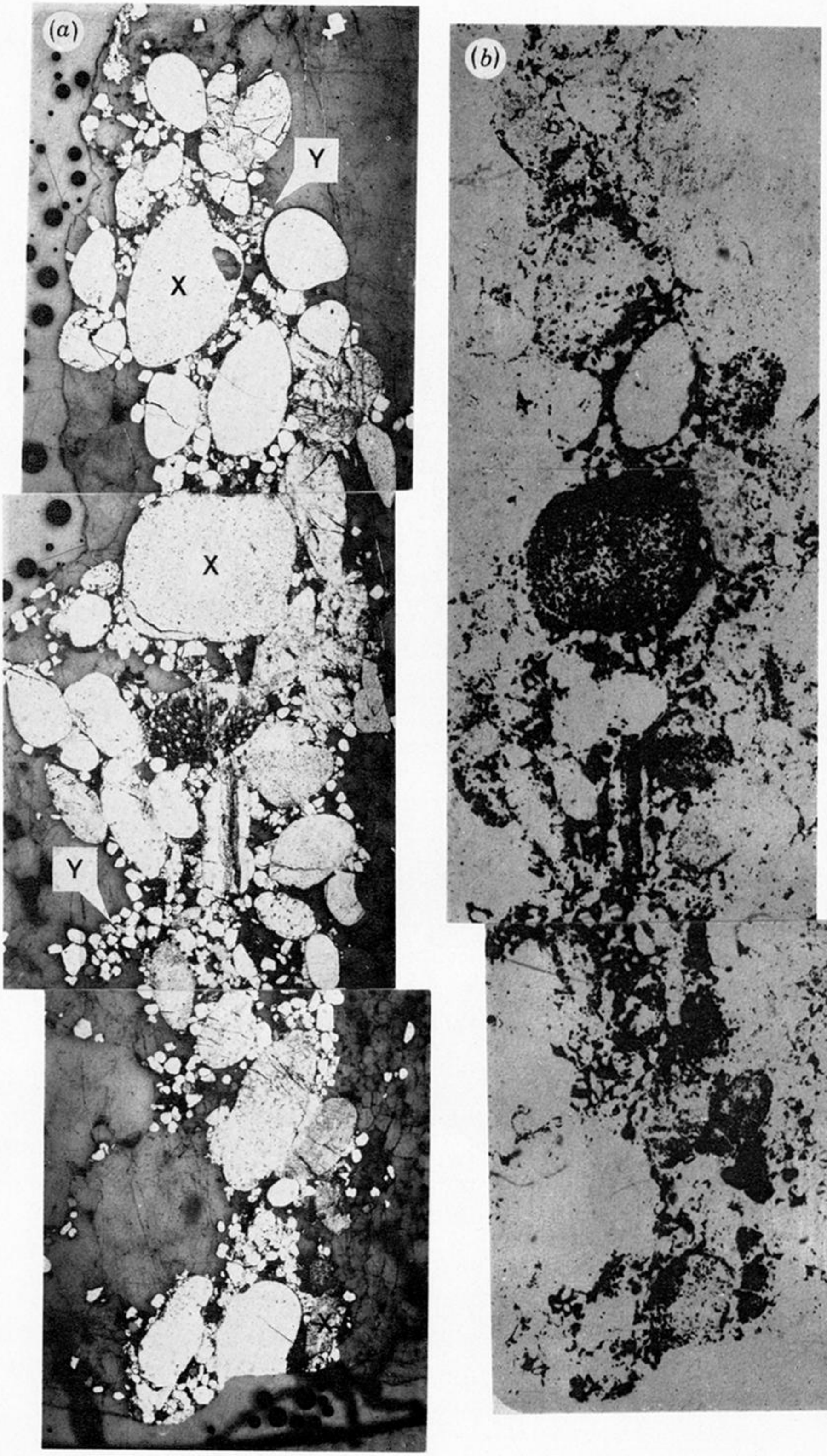

FIGURE 7. (*a*) Reflected light and (*b*) corresponding Lexan print showing uraniferous pyrite band consisting of mainly concretionary pyrite grains (white) which are a heterogeneous assemblage with regard to uranium enrichment (see Lexan print and compare grains marked *X*). Uranium present in the matrix is accounted for by the presence of allogenic grains of uraninite (*Y*) and interstitial clay minerals; Basal Reef, President Brand, Orange Free State (PTS 2463A).

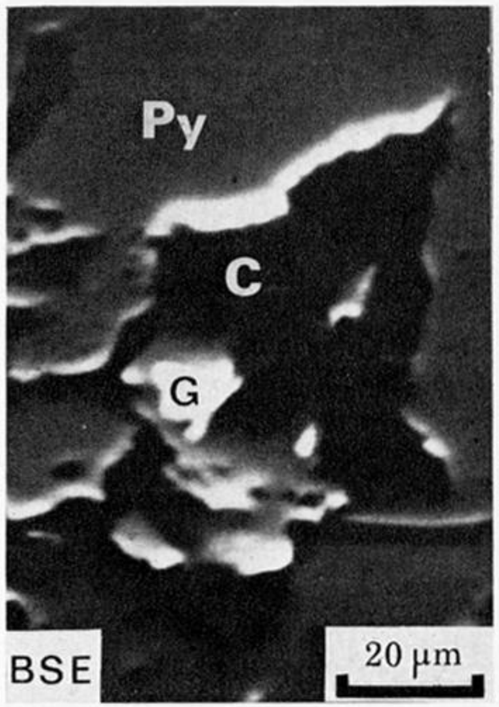

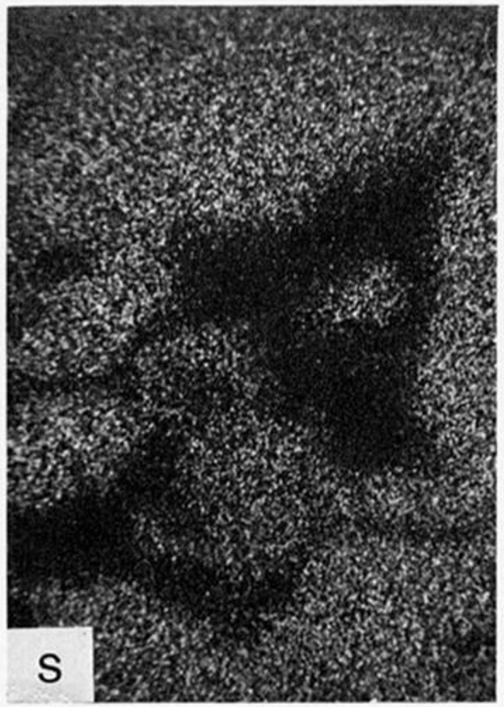

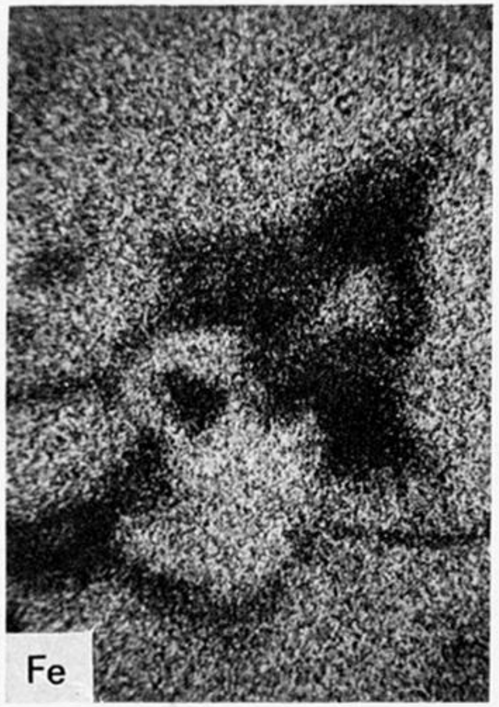

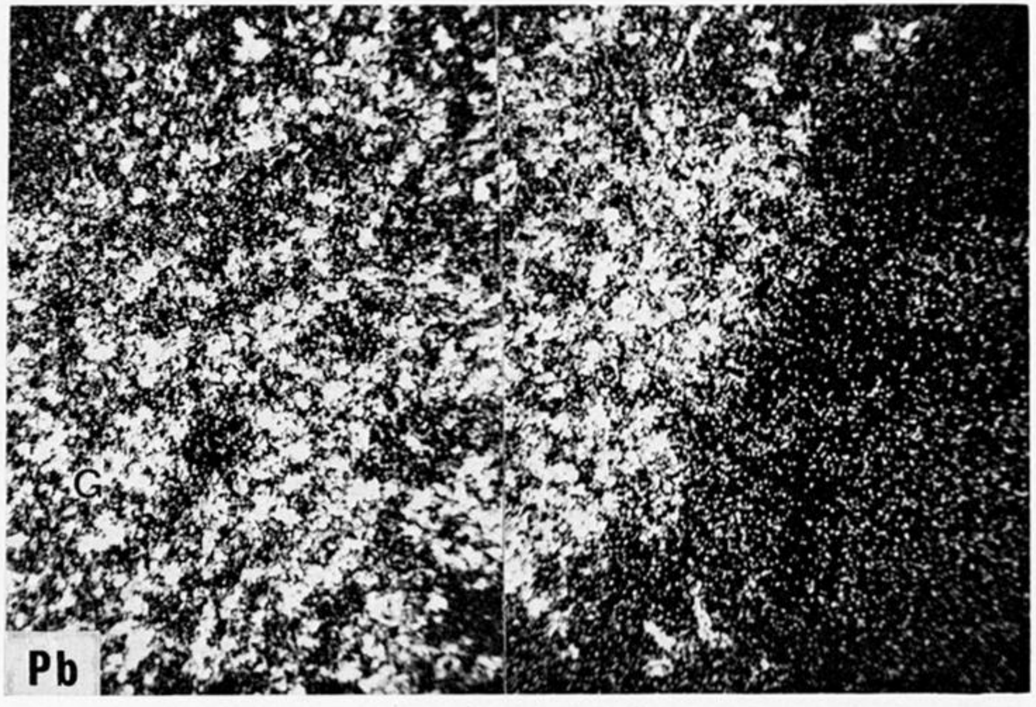

FIGURES 8 AND 9. For description see opposite.

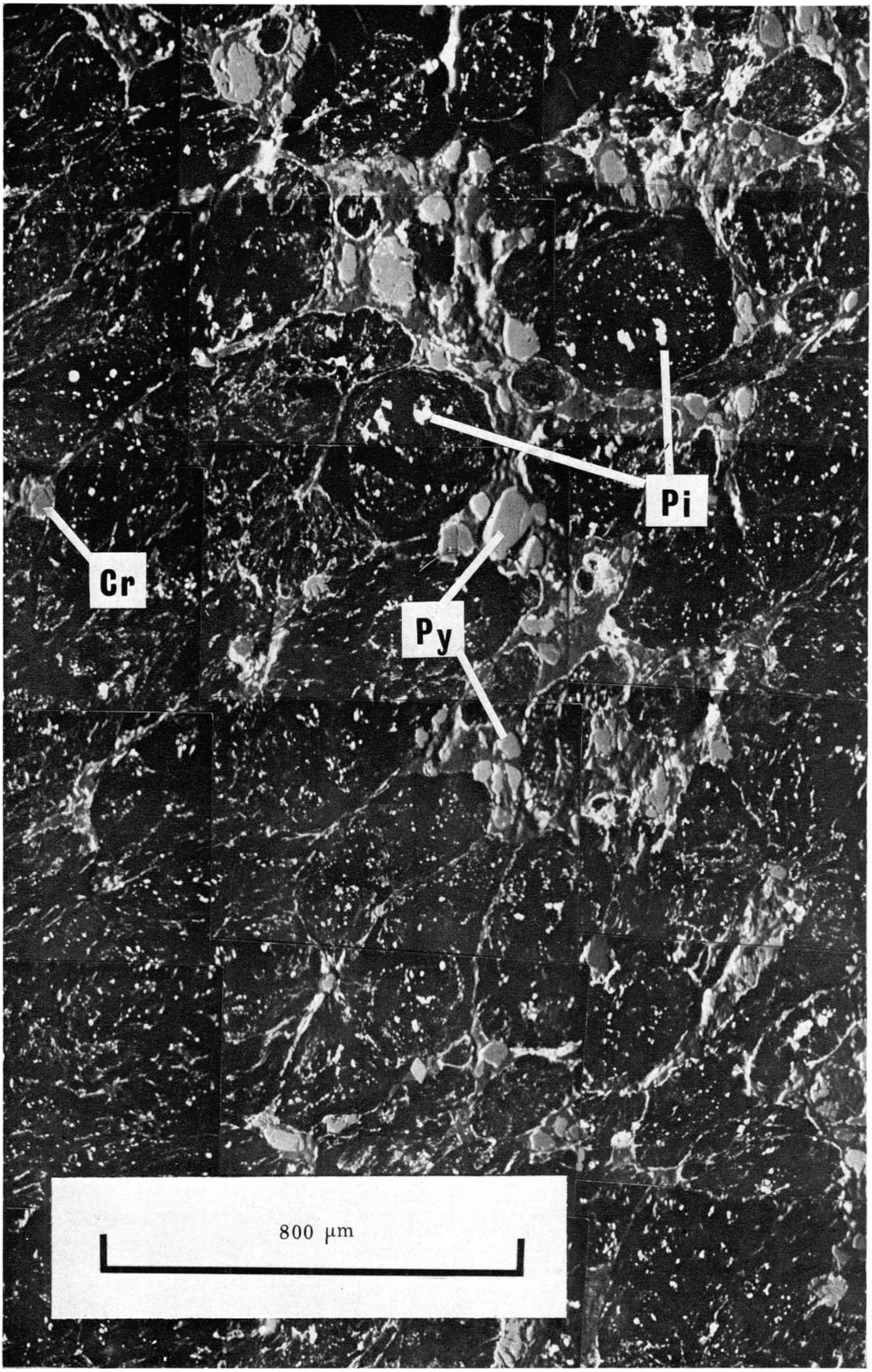

FIGURE 13. Electron probe backscattered electron image of granular carbonaceous material containing fine-grained particles of pitchblende (Pi) and gold in a carbonaceous matrix (black). Allogenic grains of pyrite (Py) and chromite (Cr) occur interstitially to the granular carbon but allogenic uraninite was not detected; Carbon Leader, West Wits (US 5).

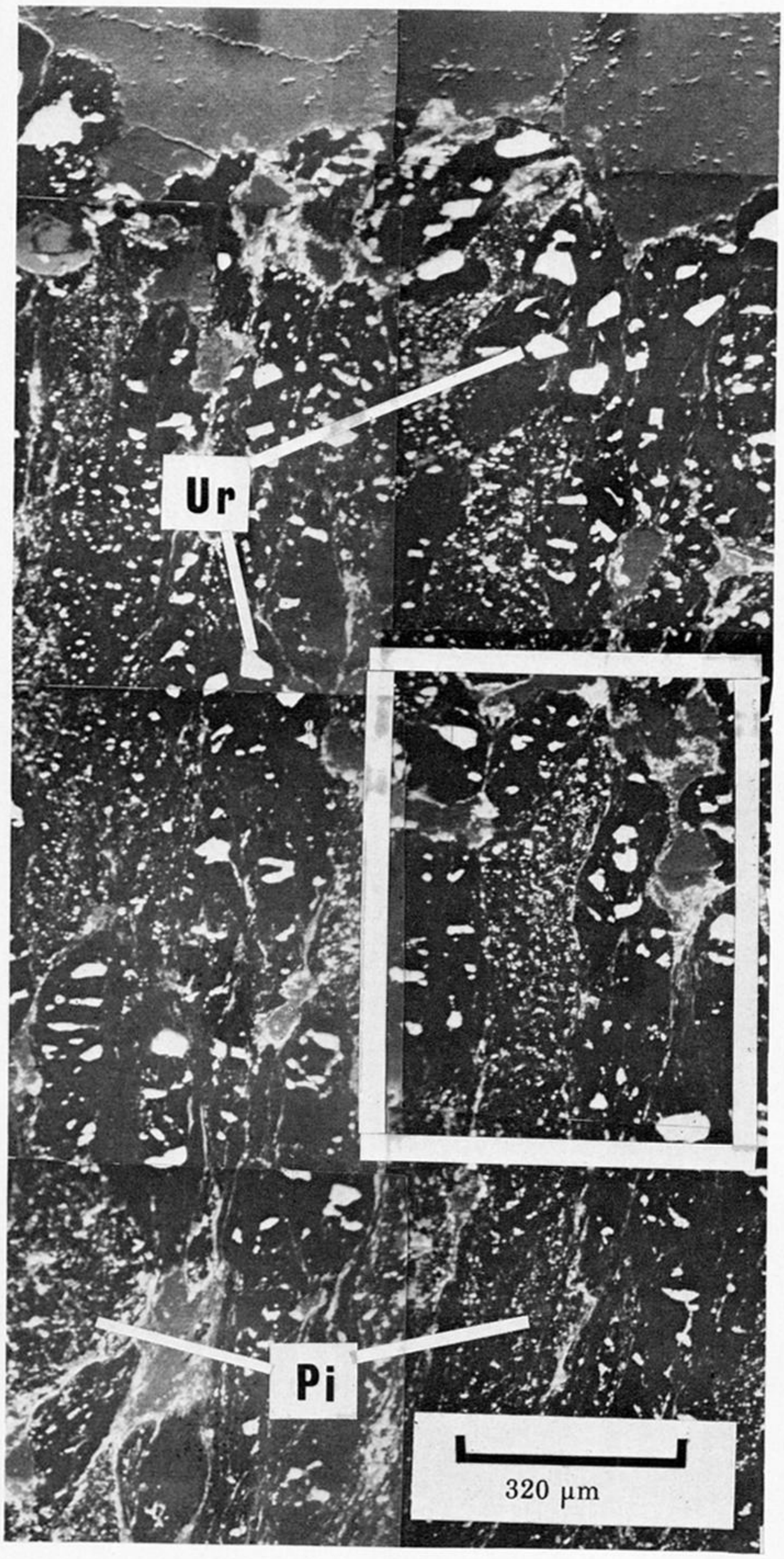

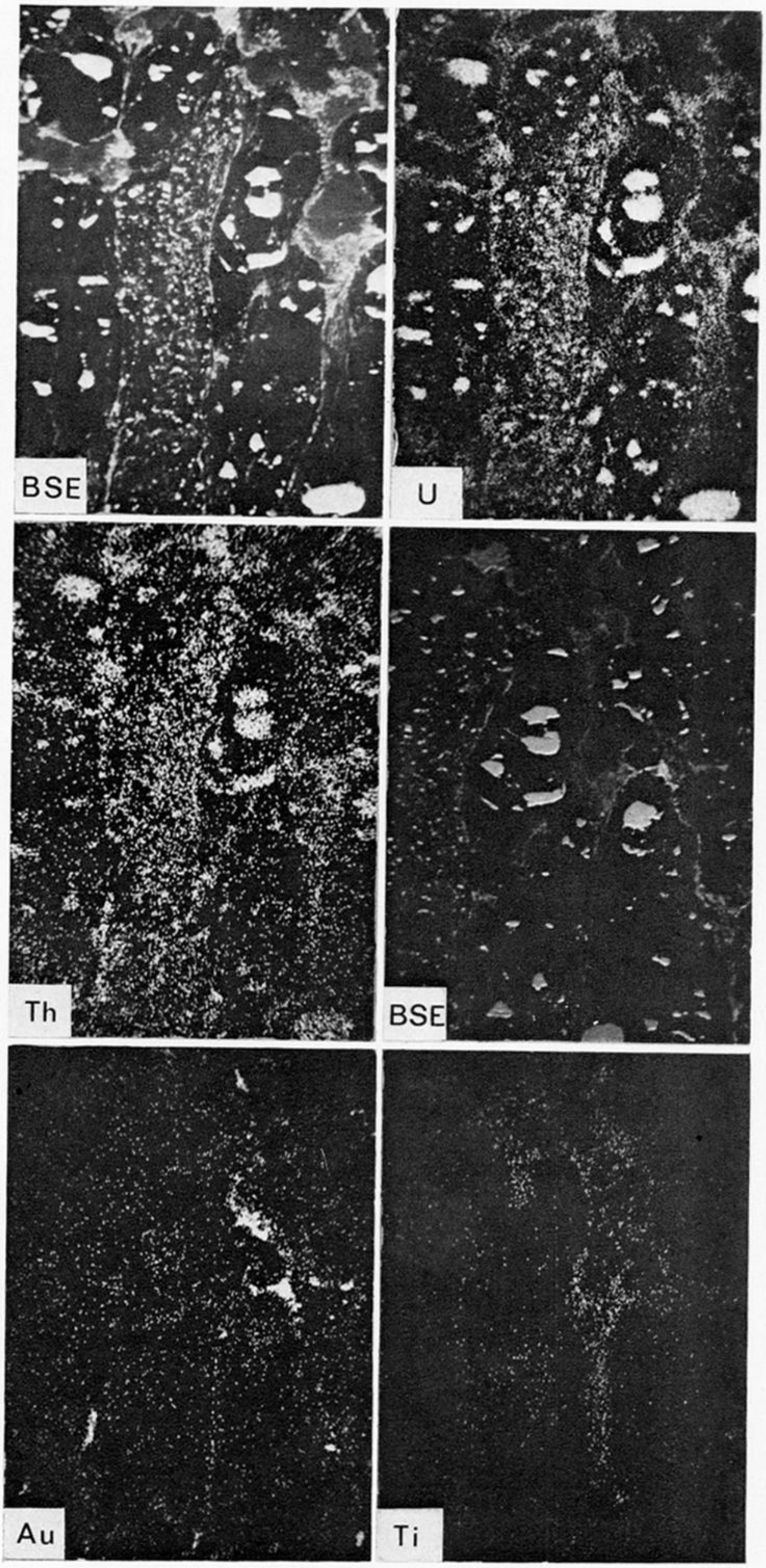

FIGURE 14. Electron-probe backscattered electron image of columnar carbon showing zones of coarse fragmented allogenic uraninite (Ur) and fine-grained disseminated pitchblende in a carbonaceous matrix (black). Vertical lineations of a strongly reflecting phase between these zones consist of fine disseminations of gold associated with brannerite, pitchblende and churchite; Vaal Reefs, Klerksdorp (PTS 2034).

FIGURE 15. Electron probe scanning images from two overlapping areas of columnar carbon within inset on figure 14 showing backscattered electron images and distribution of uranium and thorium corresponding to coarse-grained uraninite and fine-grained pitchblende. The latter is intimately associated with gold and a titaniferous phase, probably brannerite, in a carbonaceous matrix (black). Vaal Reefs, Klerksdorp (PTS 2034).

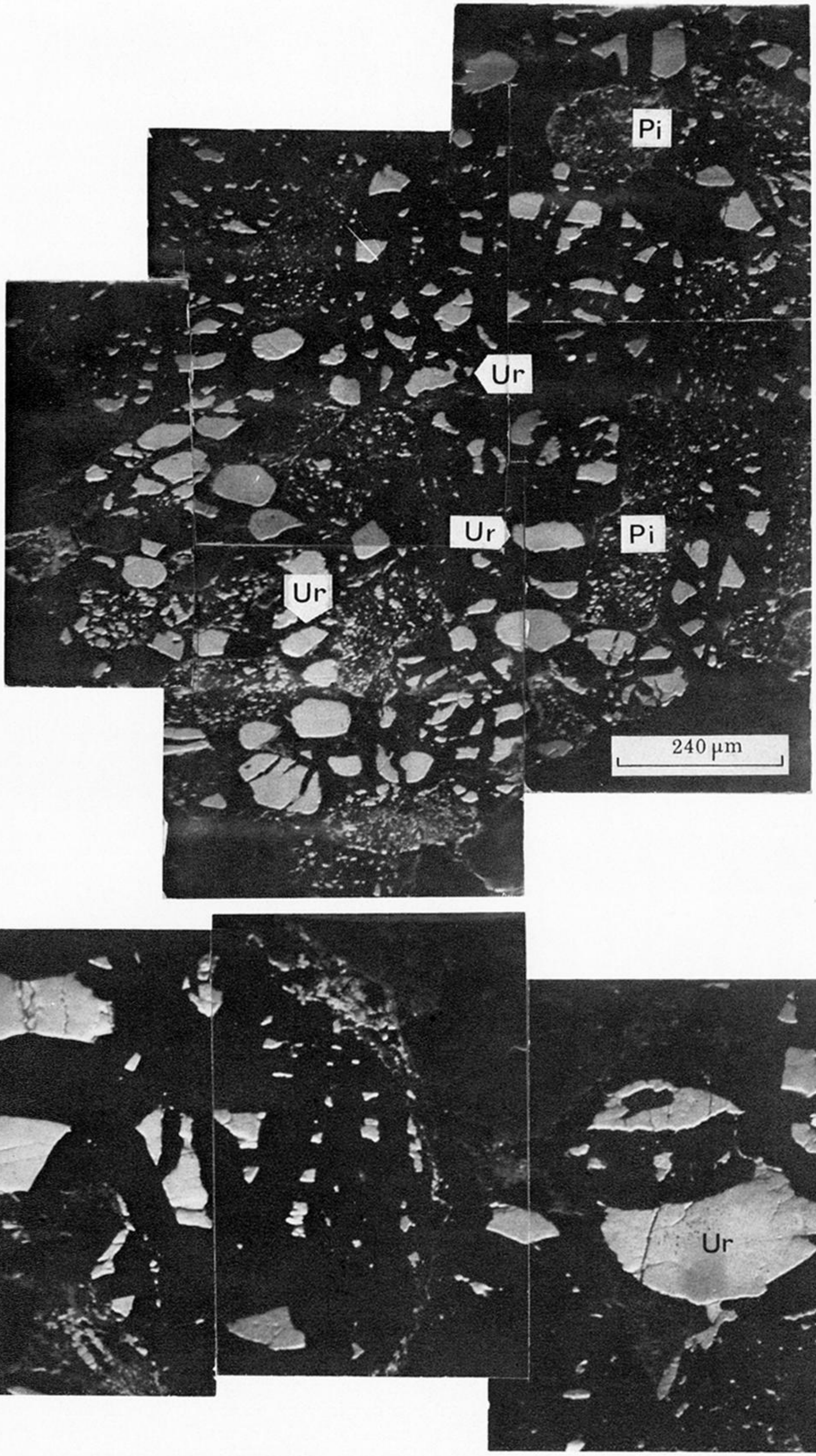

FIGURES 16 AND 17 (*a*). For description see opposite.

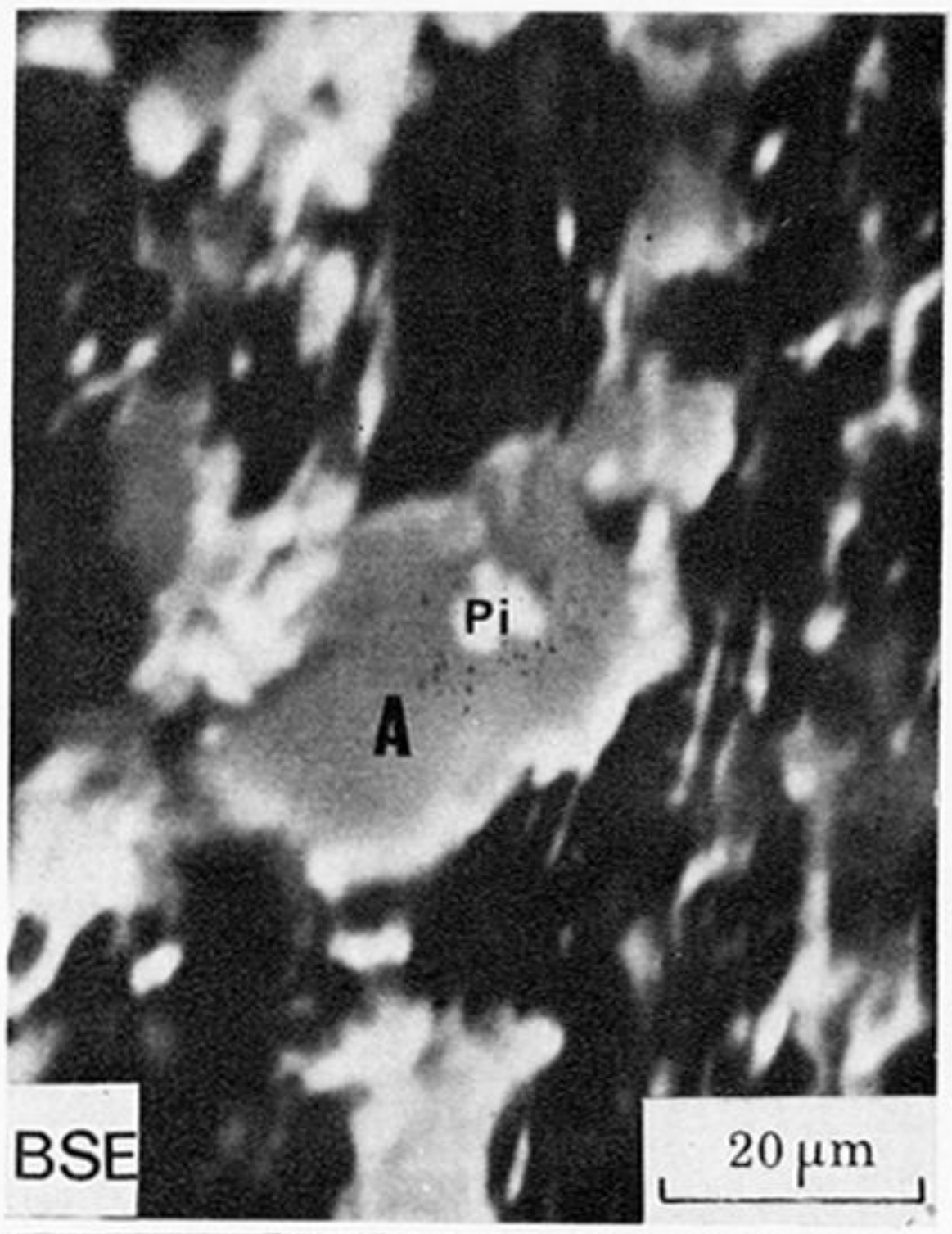

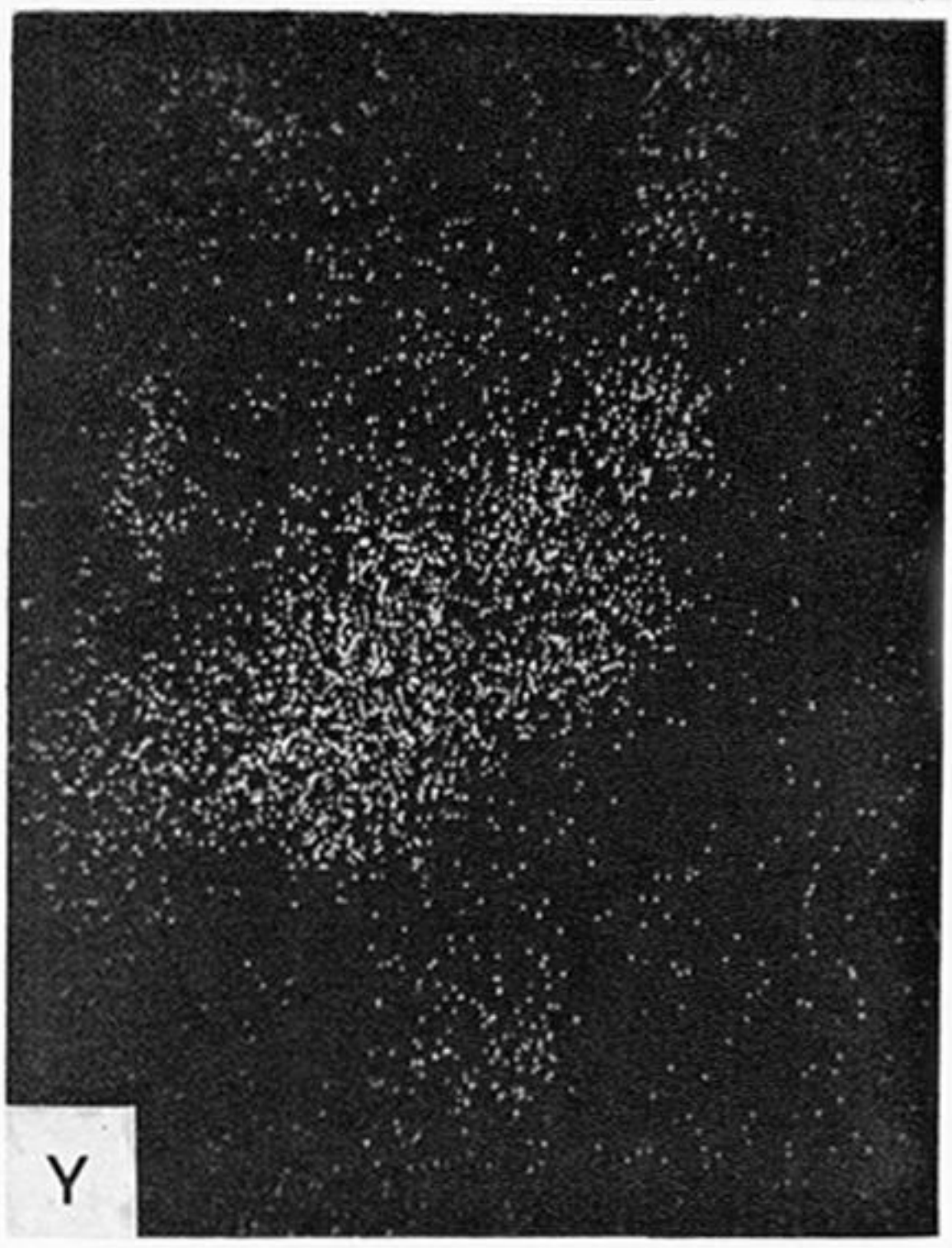

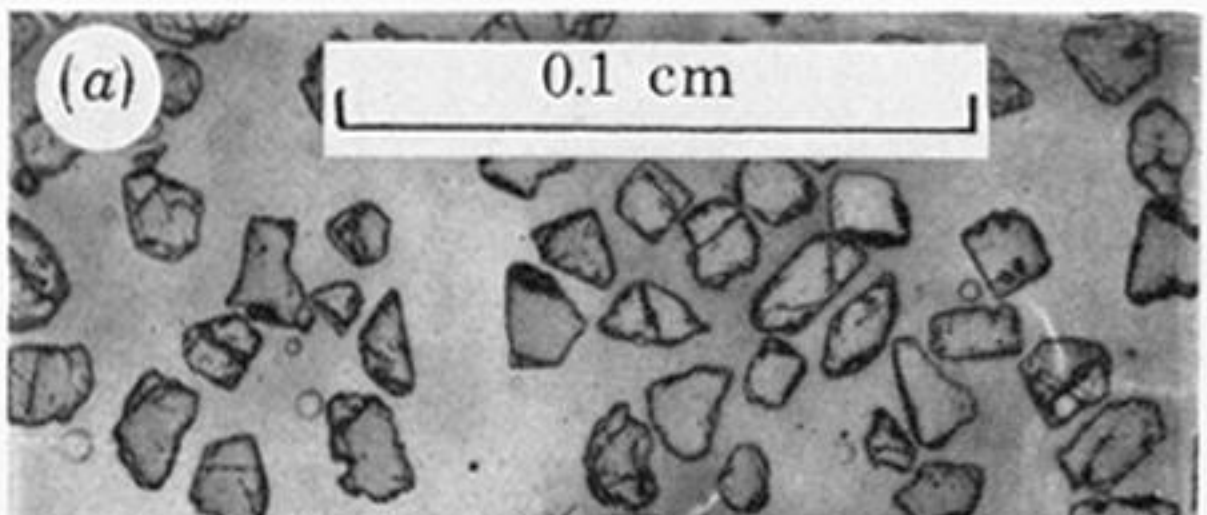

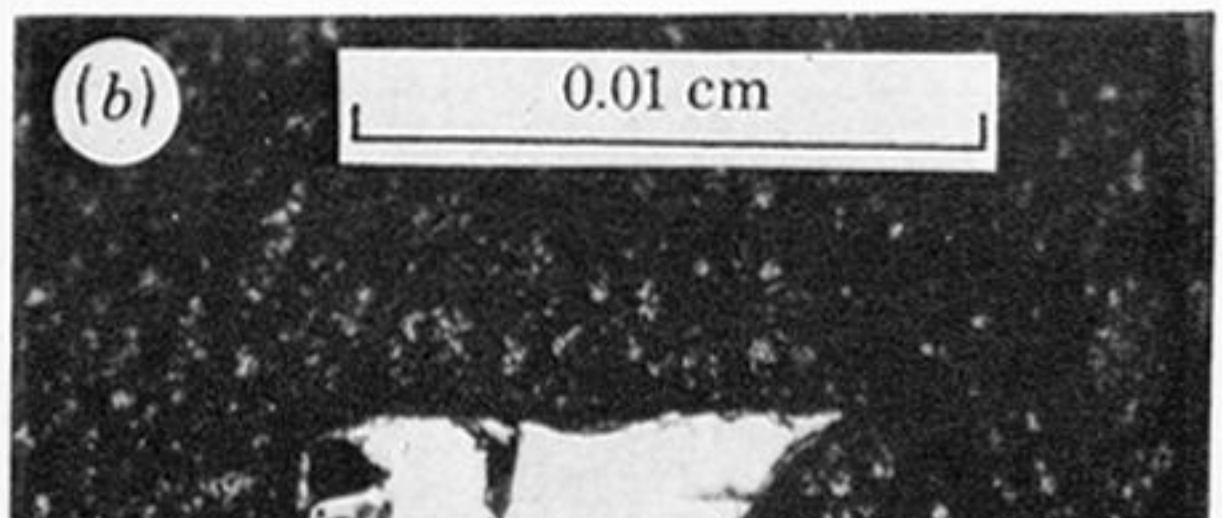

FIGURES 18 AND 19. For description see opposite.

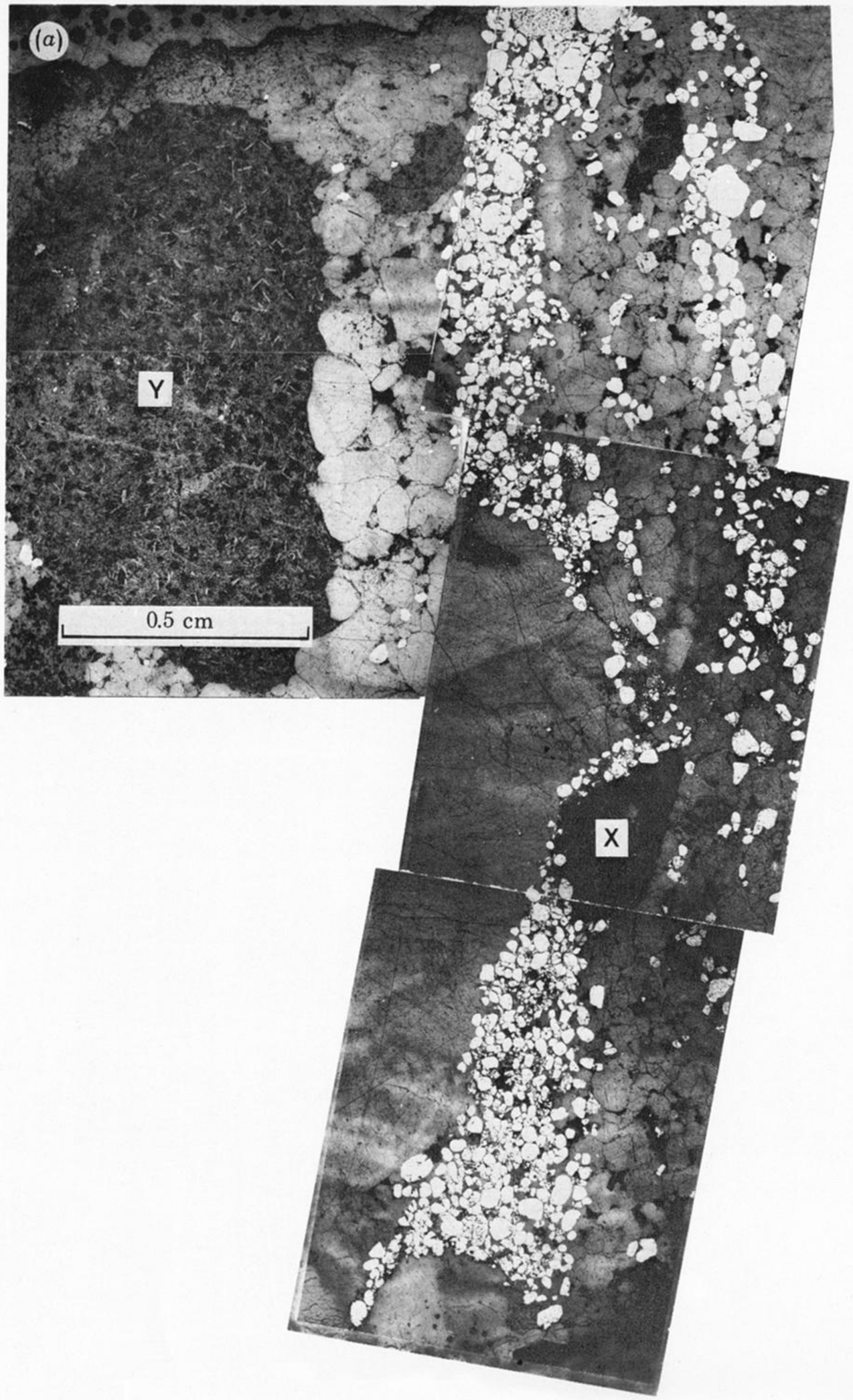
(a)
Y
X
0.5 cm

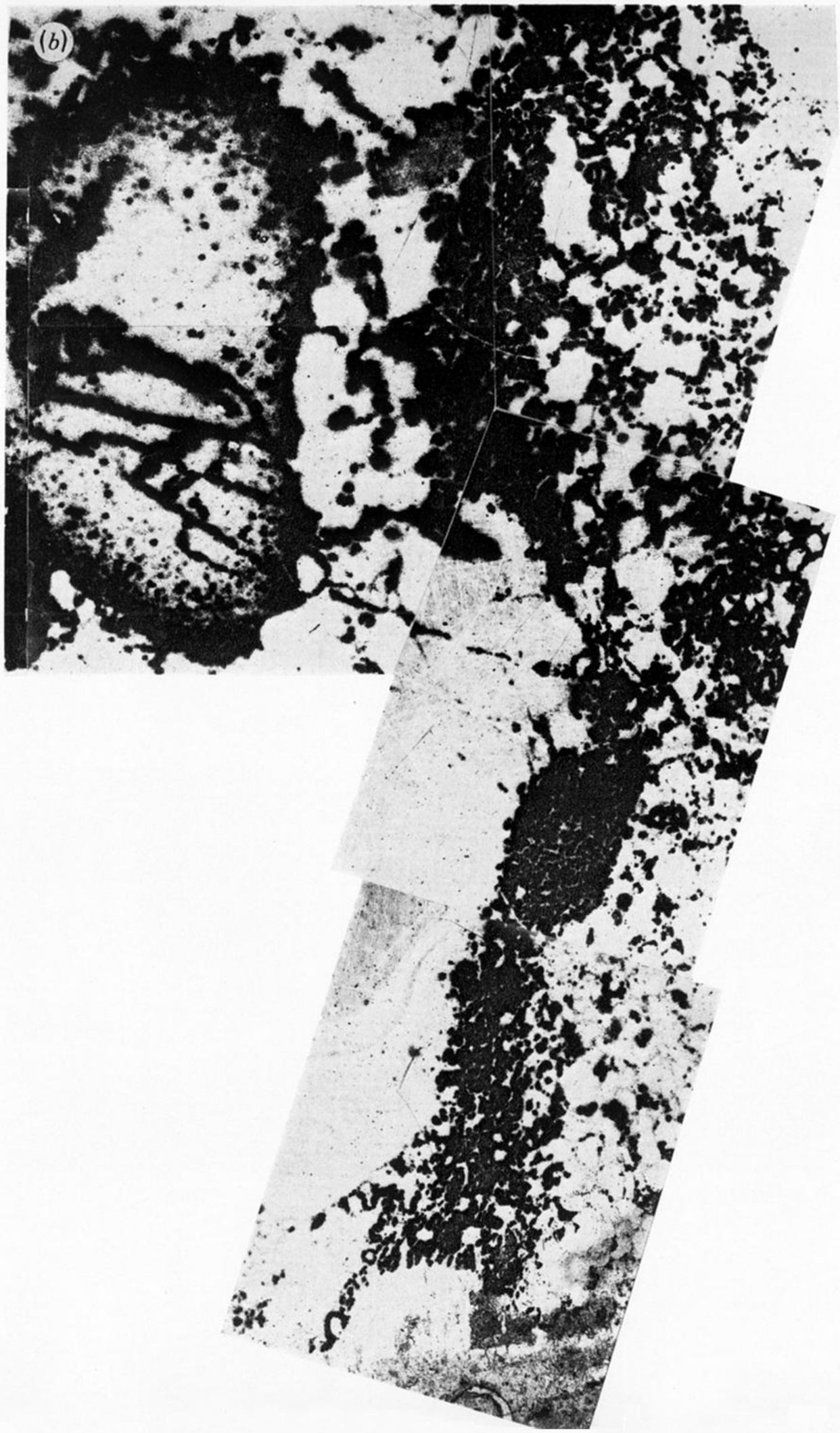
(b)